Refinements in electroweak contributions to the muon anomalous magnetic moment

Andrzej Czarnecki
Department of Physics, University of Alberta, Edmonton, Canada AB T6G 2J1

William J. Marciano
Physics Department, Brookhaven National Laboratory, Upton, New York 11973
and Institut für Theoretische Teilchenphysik, Universität Karlsruhe, D–76128 Karlsruhe, Germany

Arkady Vainshtein
Theoretical Physics Institute, University of Minnesota, 116 Church St. SE, Minneapolis, Minnesota 55455
(Received 23 December 2002; published 11 April 2003)

The effects of strong interactions on the two-loop electroweak radiative corrections to the muon anomalous magnetic moment, $a_\mu=(g_\mu-2)/2$, are examined. Short-distance logarithms are shown to be unaffected. The computation of long-distance contributions is improved by the use of an effective field theory approach that preserves the chiral properties of QCD and accounts for constraints from the operator product expansion. Small, previously neglected, two-loop contributions, suppressed by a $1-4\sin^2\theta_W$ factor, are computed and the complete three-loop leading short-distance logarithms are reevaluated. These refinements lead to a reduction in uncertainties and a slight shift in the total electroweak contribution to $a_\mu^{\rm EW}=154(1)(2)\times 10^{-11}$ where the first error corresponds to hadronic uncertainties and the second is primarily due to the allowed Higgs boson mass range.

DOI: 10.1103/PhysRevD.67.073006 PACS number(s): 13.40.Em, 14.60.Ef

I. INTRODUCTION

Recently, experiment E821 at Brookhaven National Laboratory achieved an order of magnitude improvement (relative to the classic CERN experiments) in the determination of the muon anomalous magnetic moment, $a_\mu=(g_\mu-2)/2$. The new world-average value for that fundamental quantity is [1]

$$a_\mu=116\,592\,030(80)\times 10^{-11}. \tag{1}$$

Additional data currently being analyzed should further reduce the uncertainty.

At the present level of precision, a comparison with the theoretical prediction for a_μ from the standard model requires knowledge of hadronic vacuum polarization effects with an accuracy of 1%. The most recent dispersion integral analysis [2] (see also [3]) based on data from electron-positron annihilation into hadrons and hadronic τ decays demonstrates that the issue is unsettled: e^+e^- annihilation leads to a prediction lower by about 3σ than the value (1) while the prediction based on the τ data is lower only by about 1σ. Moreover, the vector spectral functions derived from e^+e^- annihilation and from τ decays differ significantly for energies beyond the ρ resonance peak (by more than 10% in some regions). It seems very difficult to explain such a large difference by isospin breaking effects. Thus, it appears that the data from e^+e^- annihilation and from τ decays are incompatible: so, no conclusion can be derived yet about a deviation from the standard model prediction.

Since a real deviation from theory would signal the presence of "new physics," with supersymmetry the leading candidate, it is extremely important that all such hadronic uncertainties be thoroughly scrutinized and eliminated as much as possible before implications are drawn. Toward that end, new e^+e^- and τ data from Frascati and the B factories will hopefully help to resolve this puzzling difference.

Beyond the leading hadronic vacuum polarization effects, strong interaction uncertainties also enter a_μ via higher orders that involve quark loops. Quark loops appear in light-by-light scattering contributing in three loops as well as in two-loop electroweak corrections. The latter are the subject of this paper although the hadronic uncertainties there are certainly much smaller than those induced by light-by-light scattering.

At the two loop electroweak level, hadronic uncertainties arise from two types of diagrams, quark triangle diagrams related to the anomaly and hadronic photon-Z mixing. The first category has been previously studied in a free quark approximation and the more general operator product expansion. Although phenomenologically both approaches produce very close numbers they differ: particularly with regard to their explicit short distance dependence, i.e., $\log m_Z$ terms. Here, we show that this difference is due to an incomplete operator product analysis in the second approach. When corrected, unambiguous short-distance contributions result. We also take this opportunity to update the long distance and total electroweak contributions.

In the case of photon-Z mixing, its two loop contribution to a_μ is suppressed by a factor $1-4\sin^2\theta_W\sim 0.1$; so, it is not as important. It can be evaluated either in the free quark approximation (sufficient for logarithmic accuracy) or via a dispersion relation using data from e^+e^- annihilation into hadrons. The difference is shown to be numerically insignificant.

Finally, having clarified the leading short-distance behavior of the two loop electroweak radiative corrections to a_μ, we can use the renormalization group to estimate higher or-

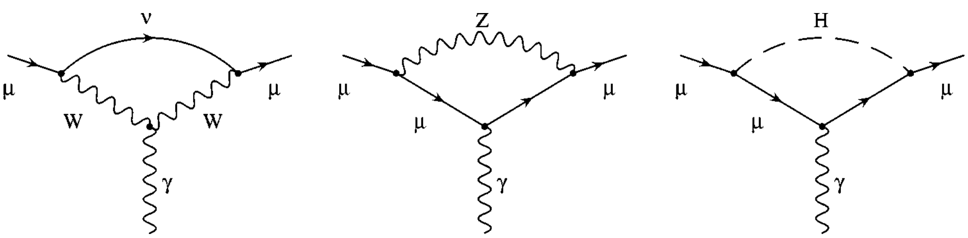

FIG. 1. One-loop electroweak contributions to a_μ.

der leading logarithm contributions which, due to an interesting cancellation, turn out to be very small.

In the end, our analysis leads to a new, not very different, but more precise and better founded prediction for the electroweak contributions to a_μ.

II. ELECTROWEAK CONTRIBUTIONS TO a_μ

In the standard model (SM) the one-loop electroweak contributions to a_μ, illustrated in Fig. 1, were computed about 30 years ago [4–8]. They have the relatively simple form

$$a_\mu^{\rm EW}\ (1\text{-loop}) = \frac{5G_\mu m_\mu^2}{24\sqrt{2}\pi^2}\left[1+\frac{1}{5}(1-4\sin^2\theta_W)^2 + \mathcal{O}\left(\frac{m_\mu^2}{m_{W,H}^2}\right)\right], \tag{2}$$

where $G_\mu = 1.16637(1)\times 10^{-5}\ \text{GeV}^{-2}$ is the Fermi constant obtained from the muon lifetime and θ_W is the weak mixing angle. For $\sin^2\theta_W$ we employ the on-shell renormalized definition

$$\sin^2\theta_W \equiv s_W^2 = 1-\frac{m_W^2}{m_Z^2}, \tag{3}$$

where $m_Z = 91.1875(21)$ GeV and the W mass is correlated with the Higgs scalar mass, m_H, via loop corrections (for $m_t = 174.3$ GeV) [9]

$$m_W = \left(80.373 - 0.05719\ln\frac{m_H}{150\ \text{GeV}} - 0.00898\ln^2\frac{m_H}{150\ \text{GeV}}\right)\ \text{GeV}. \tag{4}$$

For $m_H = 150$ GeV, the central value employed in this paper, we must use $m_W = 80.373$ GeV (rather than the direct experimental value, $m_W = 80.451(33)$ GeV, which corresponds to a very small m_H), for SM loop consistency. That implies

$$s_W^2 = 0.2231 \tag{5}$$

and

$$a_\mu^{\rm EW}(1\text{-loop}) = 194.8\times 10^{-11}. \tag{6}$$

The calculation of two-loop electroweak contributions to $a_\mu^{\rm EW}$ was more recent and considerably more involved. It started with the observation by Kukhto *et al.* [10] that some two-loop electroweak diagrams were enhanced by large logarithms of the form $\ln(m_Z/m_\mu)$. Those authors carried out detailed calculations for a number of such enhanced diagrams. They did not account, however, for closed quark loops. At about the same time, in Ref. [11] it was shown that for superheavy fermions, like the top quark, logarithms of their mass appear in corrections to magnetic moments due to triangle anomaly diagrams. Detailed studies of all closed quark loops were included in the calculation of $a_\mu^{\rm EW}$ in Refs. [12,13]. Finally, in Ref. [14], the two-loop calculation of all logarithms as well as constant terms was completed.

Two-loop corrections to $a_\mu^{\rm EW}$ naturally divide into leading logarithms (LL), i.e., terms enhanced by a factor of $\ln(m_Z/m_f)$ where m_f is a fermion mass scale much smaller than m_Z, and everything else, which we call nonleading logarithms (NLL). The two-loop leading logarithms are [see Eq. (76) below]

$$a_\mu^{\rm EW}(2\text{-loop})_{LL} = \frac{5G_\mu m_\mu^2}{24\sqrt{2}\pi^2}\cdot\frac{\alpha}{\pi}\left\{-\frac{43}{3}\left[1+\frac{31}{215}(1-4s_W^2)^2\right]\times\ln\frac{m_Z}{m_\mu} + \frac{36}{5}\sum_{f\in F} N_f Q_f\left[I_f^3 Q_f - \frac{2}{27}(I_f^3 - 2Q_f s_W^2)(1-4s_W^2)\right]\ln\frac{m_Z}{m_f}\right\}, \tag{7}$$

where $\alpha \simeq 1/137.036$, $N_f = 3$ for quarks and 1 for leptons, I_f^3 is the third component of weak isospin and Q_f is electric charge. Electron and muon loops as well as nonfermionic loops produce the $\ln(m_Z/m_\mu)$ terms in this expression (the first line) while the sum runs over $F = \tau, u, d, s, c, b$. The logarithm $\ln(m_Z/m_f)$ in the sum implies that the fermion mass m_f is larger than m_μ. For the light quarks, such as u and d, whose current masses are very small, m_f has a meaning of some effective hadronic mass scale.

In Eq. (7) we have retained for completeness small contributions from the γ-Z mixing diagrams in Fig. 2 which

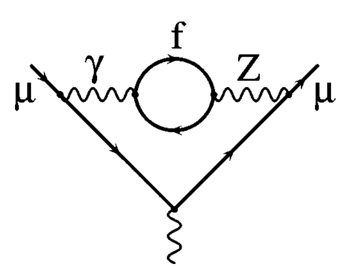

FIG. 2. Contribution to $a_\mu^{\rm EW}$ from the γ-Z mixing induced by a fermion f.

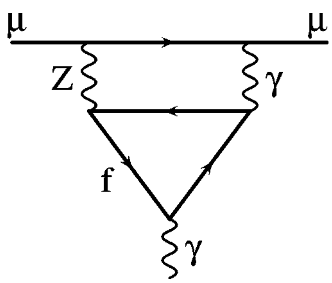

FIG. 3. Effective $Z\gamma\gamma^*$ coupling induced by a fermion triangle, contributing to $a_\mu^{\rm EW}$.

were previously excluded because they are suppressed by $(1-4s_W^2)$ for quarks and $(1-4s_W^2)^2$ for leptons.

The more important terms in Eq. (7), those not suppressed by $(1-4s_W^2)$, were checked by Degrassi and Giudice [15]. They used knowledge of well studied QCD corrections to $b\to s\gamma$ decay and translated them into into QED corrections to $a_\mu^{\rm EW}$ via appropriate coupling changes. The only place that they erred was for the small $-\frac{2}{27}(I_f^3-2Q_f s_W^2)(1-4s_W^2)\ln(m_Z/m_f)$ terms coming from quark loops. Technically the difference is due to γ-Z mixing (Fig. 2) which is proportional to $Q_f Q_\mu$ (electric charges of the loop fermion and the muon): in [15] it was given as Q_f^2.

In addition to leading logarithms, the NLL two-loop contributions have also been computed [14]. They depend on known constants, the top quark mass (here taken to be 174.3 GeV), $\ln(m_Z/m_W)$ terms, and the as yet unknown Higgs boson mass, m_H. For $m_H\simeq 150$ GeV, those corrections are numerically given by [14]

$$a_\mu^{\rm EW}(2\text{-loop})_{NLL}=-6.0\pm 1.8\times 10^{-11}, \tag{8}$$

where the error allows m_H to range from $m_H\simeq 114$ GeV (its experimental lower bound) to about 250 GeV. We have included in Eq. (8) small NLL contributions, -0.2×10^{-11}, proportional to $(1-4s_W^2)m_t^2/m_W^2$ induced by the renormalization of the weak mixing angle.

When evaluating Eq. (7), one is confronted by the presence of light u, d, and s quark masses in the logarithms. They were used to crudely regulate long distance loop contributions in Figs. 2 and 3, where QCD effects were ignored [13]. For $m_{u,d}=300$ MeV, $m_s=500$ MeV, $m_c=1.5$ GeV, and $m_b=4.5$ GeV, one finds

$$a_\mu^{\rm EW}(2\text{-loop})_{LL}=-(36.7\pm 2)\times 10^{-11}, \tag{9}$$

where the error is meant to roughly reflect low-momentum hadronic loop uncertainties for the u, d, and s quarks in Fig. 3. Together, Eqs. (8) and (9) provide the two-loop total electroweak correction $a_\mu^{\rm EW}(2\text{-loop})=-42.7(2)(1.8)\times 10^{-11}$, which together with Eq. (6) leads to the generally quoted standard model prediction [16],

$$a_\mu^{\rm EW}=152(4)\times 10^{-11}, \tag{10}$$

where the error of $\pm 4\times 10^{-11}$ is meant to reflect the total uncertainties coming from hadronic loop effects, the unknown Higgs mass, and uncalculated higher order (three-loop) contributions.

Refinements in the above analysis are possible on two fronts: improvement in the low-momentum contribution of hadronic loops and an estimation of the leading three-loop electroweak contribution (which is part of the overall uncertainty). The Higgs mass uncertainty will be overcome with its discovery.

The easiest hadronic loop improvement can be made in the quark contributions to γ-Z mixing pictured in Fig. 2. Those effects, embodied in the last part of the bracketed terms in Eq. (7) can be obtained via a dispersion relation using $\sigma(e^+e^-\to\text{hadrons})$ data. Such an analysis has been performed for various low energy processes. It effectively leads to the replacement [17]

$$-\frac{2}{3}\sum_{q=u,d,s,c,b} N_q(I_q^3 Q_q-2Q_q^2 s_W^2)\ln\frac{m_Z}{m_q}\to -6.88\pm 0.50 \tag{11}$$

which is somewhat larger than the value (-5.95) obtained in logarithmic approximation with constituent u, d, and s quark masses. (It suggests that smaller quark masses might be more appropriate.) Because those γ-Z mixing effects are suppressed by $1-4s_W^2$, the shift in $a_\mu^{\rm EW}$ from this modification is tiny, -0.02×10^{-11}, and can be safely neglected.

Low momentum loop effects in the light quark triangle diagrams of Fig. 3 are more important. It is clear that the use of an effective quark mass as an infrared cutoff is in contradiction with the chiral properties of QCD in the case of light quarks. Indeed, in the chiral limit the infrared singularity in the quark triangle does not go away: it matches the Goldstone pole in hadronic terms. This refers to the anomalous part of the triangle, i.e., to the longitudinal part of the axial current.

The issue of how to properly treat light quark triangle diagrams was addressed originally in a study by Peris, Perrotet, and de Rafael [12] within a low-energy effective field theory approach for π, η, and η' mesons. More recently, Knecht, Peris, Perrotet and de Rafael [18] have reexamined the issue using an operator product expansion (OPE) and Ward identities as guidance. We find their approach to the anomaly related longitudinal part of quark triangles to be a valid improvement over the naive constituent quark mass cutoff of Eq. (7).

Unfortunately, their rather sophisticated OPE analysis failed to properly address the short-distance behavior of nonanomalous, i.e., transversal, part of the light quark triangles in Fig. 3. In particular, they do not reproduce the complete $\ln m_Z$ terms in Eq. (7). That difference was attributed to QCD damping effects in [18] which were claimed to eliminate the nonanomalous $\ln m_Z$ light quark contributions. However, in our opinion, it points to a shortcoming in their analysis.

In Sec. III we address in some detail what modifications to the study in [18] are required to restore the proper short-distance behavior. We then employ the effective field theory approach to improve the evaluation of light quark diagrams in Fig. 3, thus refining their contribution to $a_\mu^{\rm EW}$.

Having verified the short-distance behavior of Eq. (3) we are also in a position to evaluate higher order leading logarithms via the renormalization group. That analysis is carried out in Sec. IV, where the leading logarithm three-loop contributions to $a_\mu^{\rm EW}$ are determined. Such a study was previously undertaken by Degrassi and Giudice [15]. Although we find small differences with their analysis, in the end we also obtain a very small leading logarithm three-loop contribution to $a_\mu^{\rm EW}$. In fact, the result is consistent with zero, to our level of accuracy, due to an interesting cancellation between anomalous dimensions and beta function effects.

Finally, in Sec. V, we give a refined determination of $a_\mu^{\rm EW}$ for which the errors are reduced and the central value is slightly shifted due to improvements in our analysis.

III. HADRONIC EFFECTS IN QUARK TRIANGLES

An interesting subset of the two-loop contributions to $a_\mu^{\rm EW}$ are those containing fermionic triangles of quarks and leptons, see Fig. 3. The internal triangles define the one-loop $Z^*\gamma\gamma^*$ amplitude where the Z and one photon are virtual while the other photon is real and soft. Those same triangles produce the well-known anomaly part of the Z boson axial current. For cancellation of the anomaly, one needs to sum over all fermions in a given generation.

In the case of $a_\mu^{\rm EW}$, the cancellation between quarks and leptons in Fig. 3 is not complete because of their different masses and interactions. In this section we give a detailed analysis of the general structure of the $Z^*\gamma\gamma^*$ amplitude, paying particular attention to the effect of strong interactions on the quark diagrams. Perturbative QCD corrections to short-distance logarithms are shown to vanish and have an overall negligible effect for heavy quark diagrams. In the case of light quarks, an operator product expansion and effective field theory approach are used to improve the evaluation of long-distance QCD effects. These refinements lead to an update of the fermionic triangle loop contributions to $a_\mu^{\rm EW}$.

A. Structure of the $Z^*\gamma\gamma^*$ interaction

We begin our general analysis by introducing some definitions. The interaction Lagrangian for the electromagnetic and Z-boson fields, A_μ and Z_ν, is

$$\mathcal{L}_{\rm int}=eA^\mu j_\mu-\frac{g}{4\cos\theta_W}Z^\nu j_\nu^5, \qquad j_\mu=\sum_f Q_f\bar f\gamma_\mu f,\quad j_\nu^5=\sum_f 2I_f^3\bar f\gamma_\nu\gamma_5 f, \tag{12}$$

where Q_f and I_f^3 are the electric charge and the third component of weak isospin and we retain only the axial part of the Z-boson current. (The weak vector current contribution in Fig. 3 vanishes by Furry's theorem.)

The $Z^*\gamma\gamma^*$ amplitude $T_{\mu\nu}$ is defined as

$$T_{\mu\nu}=i\int d^4x e^{iqx}\langle 0|T\{j_\mu(x)j_\nu^5(0)\}|\gamma(k)\rangle. \tag{13}$$

That is equivalent to

$$T_{\mu\nu}=ee^\gamma T_{\mu\gamma\nu}, \qquad T_{\mu\gamma\nu}=-\int d^4x\, d^4y\, e^{iqx-iky}\langle 0|T\{j_\mu(x)j_\gamma(y)j_\nu^5(0)\}|0\rangle, \tag{14}$$

where e^γ is the photon polarization vector. We consider the limit of small photon momentum k. The expansion of $T_{\mu\nu}$ in k starts with linear terms and we neglect quadratic and higher powers of k. In this approximation there are two Lorentz structures for $T_{\mu\nu}$ consistent with electromagnetic current conservation,

$$T_{\mu\nu}=-\frac{ie}{4\pi^2}[w_T(q^2)(-q^2\tilde f_{\mu\nu}+q_\mu q^\sigma\tilde f_{\sigma\nu}-q_\nu q^\sigma\tilde f_{\sigma\mu})+w_L(q^2)q_\nu q^\sigma\tilde f_{\sigma\mu}], \qquad \tilde f_{\mu\nu}=\frac{1}{2}\epsilon_{\mu\nu\gamma\delta}f^{\gamma\delta},\quad f_{\mu\nu}=k_\mu e_\nu-k_\nu e_\mu. \tag{15}$$

The first structure is transversal with respect to the axial current index ν, the second is longitudinal.

The contribution of $Z^*\gamma\gamma^*$ to the muon anomalous magnetic moment $a_\mu^{\rm EW}$ in the unitary gauge where the Z propagator is $i(-g_{\mu\nu}+q_\mu q_\nu/m_Z^2)/(q^2-m_Z^2)$, can be written in terms of $w_{T,L}(q^2)$ as

$$\Delta a_\mu^{\rm EW}=\frac{\alpha}{\pi}2\sqrt{2}G_\mu m_\mu^2 i\int\frac{d^4q}{(2\pi)^4}\frac{1}{q^2+2qp}\left[\frac{1}{3}\left(1+\frac{2(qp)^2}{q^2m_\mu^2}\right)\times\left(w_L-\frac{m_Z^2}{m_Z^2-q^2}w_T\right)+\frac{m_Z^2}{m_Z^2-q^2}w_T\right]. \tag{16}$$

Here p is the four-momentum of the external muon. For logarithmic estimates, a much simpler expression is sufficient:

$$\Delta a_\mu^{\rm EW}=\frac{\alpha}{\pi}\frac{G_\mu m_\mu^2}{8\pi^2\sqrt{2}}\int_{m_\mu^2}^\infty dQ^2\left(w_L+\frac{m_Z^2}{m_Z^2+Q^2}w_T\right), \tag{17}$$

where $Q^2=-q^2$. Moreover, the same expression with the lower limit of integration set to zero works with a power accuracy (in m_μ^2/m_f^2) in the case of a heavy fermion in the loop, $m_f\gg m_\mu$.

The one-loop results for $Z^*\gamma\gamma^*$ can be taken from the classic papers by Adler [19] and Rosenberg [20]. In Ref. [10] they were considerably simplified in the limit of small external photon momentum. One then finds the following one-loop expressions for invariant functions $w_{L,T}$,

$$w_L^{\text{1-loop}}=2w_T^{\text{1-loop}}=\sum_f\ 4I_f^3N_fQ_f^2\int_0^1\frac{\mathrm{d}\,\alpha\alpha(1-\alpha)}{\alpha(1-\alpha)Q^2+m_f^2}, \tag{18}$$

where the factor N_f accounts for colors in the case of quarks.

We also independently calculated $T_{\mu\nu}$ using Schwinger operator methods for the fermionic loop. It can be presented as the polarization operator describing the mixing of two currents, j_μ and j_ν^5, but with the fermion propagators taken in the external field with the constant field strength. In the fixed point gauge $x^\mu A_\mu=0$ this propagator has the form [21]

$$S(p)=\frac{1}{\not p-m}+\frac{1}{(p^2-m^2)^2}eQ\tilde{F}_{\rho\delta}\left(p^\rho\gamma^\delta-\frac{i}{2}m\sigma^{\rho\delta}\right)\gamma_5 +\mathcal{O}(F^2). \tag{19}$$

Then straightforward calculations lead to the above expressions (18) for the invariant functions $w_{T,L}(q^2)$.

The corresponding two-loop contributions to a_μ^{EW} were calculated in Refs. [12,13]. According to Eq. (16) one needs to integrate using the $w_{T,L}$ given in Eq. (18). Let us consider the part $w_{T,L}[f]$ which is due to the loop of a given fermion f with the mass m_f at the range of $Q^2\gg m_f^2$. The asymptotic behavior of $w_{T,L}[f]$ at large Q^2 is

$$w_L^{\text{1-loop}}[f]=2w_T^{\text{1-loop}}[f] =4I_f^3N_fQ_f^2\left[\frac{1}{Q^2}-\frac{2m_f^2}{Q^4}\ln\frac{Q^2}{m_f^2}+\mathcal{O}\left(\frac{1}{Q^6}\right)\right]. \tag{20}$$

At large Q^2 we can use the simpler form (17) for integration. It is clear then that for the individual fermion loop the integral $\int \mathrm{d}Q^2 w_L$ is divergent. This reflects the fact that the theory is inconsistent unless the condition of anomaly cancellation between leptons and quarks is fulfilled. This condition has the form

$$\sum_f\ I_f^3N_fQ_f^2=0 \tag{21}$$

within every generation. It means that at $Q^2\gg m_f^2$ the leading terms $1/Q^2$ cancel out after summing over fermions and $w_L \sim(\ln Q^2)/Q^4$ implying convergence for a_μ^{EW}.

Note the difference between the w_L and w_T parts in the integral (17). The first one does not depend on m_Z at all while for the second we have a cutoff factor $1/(Q^2+m_Z^2)$. Therefore, the w_T part is never divergent, instead individual fermion loops produce $\log(m_Z/m_f)$ terms in a_μ^{EW} when $m_f \ll m_Z$. On the other hand, the one-loop relation $w_T=w_L/2$ means the anomaly cancellation condition (21) leads to cancellation of the leading $1/Q^2$ terms in w_T as well. It results in the absence of $\log m_Z$ terms when $m_f\ll m_Z$ for all fermions in the given generation.

B. Hadronic corrections for quark triangles

How good is the one-loop approximation for w_L and w_T? This question pertains to strong interaction effects for quark loops. As characterized in [12] this issue brings about a new class of hadronic contributions to the muon anomalous magnetic moment.

Let us first discuss perturbative corrections to the $Z\gamma\gamma^*$ amplitude at $Q\gg m_q$ due to gluon exchange in quark loops. The longitudinal function w_L is protected against these corrections by a nonrenormalization theorem [22] for the anomaly. What about the transversal function w_T? If the α_s corrections were present for w_T then after summing over the fermion generation, the leading term would become $\alpha_s(Q)/Q^2\sim 1/(Q^2\log Q/\Lambda_{\text{QCD}})$. According to Eq. (17) this leads to terms in a_μ^{EW} which are parametrically enhanced by $\log(\log m_Z/\Lambda_{\text{QCD}})$.

It turns out, however, that the α_s corrections in w_T are also absent at $Q\gg m_q$ due to the new nonrenormalization theorem proved in Ref. [23]. The proof, stimulated by the present study, is based on preservation of the relation $w_T =w_L/2$ beyond the one loop, i.e., in the presence of QCD interactions. This relation holds only for the specific kinematics we consider in which the external photon momentum is vanishing.

Our above discussion means that α_s corrections are absent for both w_L and w_T in the chiral limit $m_q=0$. When quarks are heavy the α_s corrections can appear but with a suppression factor m_q^2/Q^2 at $Q\gg m_q$. In application to a_μ^{EW} it implies that perturbative α_s corrections are absent for light quarks. For heavy quarks, the logarithmic terms which are due to $Q\gg m_q$ are not renormalized but nonlogarithmic terms regulated by $\alpha_s(m_q)$ could appear due to the range of momenta $Q\sim m_q$.

Next comes the question of nonperturbative corrections. For the heavy quarks these corrections, given by some power of $\Lambda_{\text{QCD}}^2/m_q^2$, are small. As discussed above, the perturbative strong interaction corrections governed by $\alpha_s(m_q)$ are also small for heavy quarks. In particular, this argument is applicable to the third generation, τ, b, and t loops, so the free quark computational results obtained in Refs. [12,13,18] are very much under theoretical control.

The first and the second generations contain light quarks u,d,s for which the momentum range of Q spans the hadronic scale Λ_{QCD} where nonperturbative effects are $\mathcal{O}(100\%)$ and give unsuppressed contributions to a_μ^{EW}. This problem has been addressed in the literature and two approaches were suggested. In Ref. [13] effective quark masses for light quarks in one-loop expressions were introduced as a simple way to account for strong interactions. This mass plays the role of an infrared cutoff in the integral over Q. A more realistic approach to the relevant hadronic dynamics was worked out in Refs. [12,18]. Unfortunately, some conceptual mistakes in applying the OPE (we are going to comment on them in more detail in Sec. III E) led to incorrect results. This is immediately obvious in the ultraviolet sensitivity of the results in Ref. [18]: the dependence on $\ln m_Z$ is not suppressed for the first and the second generations where all the masses are much less than m_Z.

For light quarks nonperturbative corrections to $Z\gamma\gamma^*$ are given by powers of $\Lambda^2_{\rm QCD}/Q^2$ while perturbative ones are absent as we discussed above. Thus, in the range of Q of order m_Z the one-loop perturbative approach applies and suppression of the dependence on m_Z due to the cancellation of the $\log m_Z$ terms for $a_\mu^{\rm EW}$ between leptons and quarks in the first two generations is guaranteed.

The actual interplay of nonperturbative effects for light quark contributions to $a_\mu^{\rm EW}$ represents an interesting picture very different for the longitudinal w_L and transversal w_T parts. For the first generation, in the chiral limit ($m_{u,d}=0$) nonperturbative effects are absent in w_L and the $1/Q^2$ one-loop behavior in hadronic terms matches the massless pion pole. This is the 't Hooft matching condition [24], as was pointed out in [12,18]. However, nonperturbative effects are crucial for w_T, where they are responsible for a transformation of the $1/Q^2$ singularity at small Q into ρ and a_1 meson poles.

The situation is similar but somewhat more cumbersome for the s quark in the second generation due to the U(1) anomaly (the η' meson should be included together with η meson). Also chiral breaking effects due to m_s are more important.

Below we present a detailed discussion of perturbative and nonperturbative effects for different generations.

C. Third generation effect for $a_\mu^{\rm EW}$

As we discussed above the one-loop expressions in Eq. (18) work very well for the third generation where both perturbative and nonperturbative corrections due to strong interactions are small. Substituting $w_{L,T}$ from Eq. (18) into Eq. (17) we get, for the sum of τ, b, and t contributions to $a_\mu^{\rm EW}$, the following result [12,13,18]:

$$\Delta a_\mu^{\rm EW}[\tau,b,t]=-\frac{\alpha}{\pi}\frac{G_\mu m_\mu^2}{8\pi^2\sqrt{2}}\left[\frac{8}{3}\ln\frac{m_t^2}{m_Z^2}-\frac{2}{9}\frac{m_Z^2}{m_t^2}\left(\ln\frac{m_t^2}{m_Z^2}+\frac{5}{3}\right)\right.$$
$$\left.+4\ln\frac{m_Z^2}{m_b^2}+3\ln\frac{m_b^2}{m_\tau^2}-\frac{8}{3}\right], \tag{22}$$

where we neglected small corrections of order $m_\mu^2/m^2_{\tau,b,t,Z}$, $m^2_{\tau,b}/m_Z^2$, and m_Z^4/m_t^4. Numerically,

$$\Delta a_\mu^{\rm EW}[\tau,b,t]=-\frac{\alpha}{\pi}\frac{G_\mu m_\mu^2}{8\pi^2\sqrt{2}}\cdot 30.3=-8.21\times 10^{-11}, \tag{23}$$

which is properly included in the results of Eqs. (7) and (8).

Following the discussion in Sec. III B, we estimate a perturbative uncertainty by adding terms of order of $\alpha_s(m_q)/\pi$ to $\log m_q$. It gives for the uncertainty

$$-\frac{\alpha}{\pi}\frac{G_\mu m_\mu^2}{8\pi^2\sqrt{2}}\left\{\frac{16}{3}C_t\frac{\alpha_s(m_t)}{\pi}-2C_b\frac{\alpha_s(m_b)}{\pi}\right\}, \tag{24}$$

where C_t and C_b are numbers of order ± 1. Using $\alpha_s(m_Z)=0.11$, we come to an estimate

$$\pm\frac{\alpha}{\pi}\frac{G_\mu m_\mu^2}{8\pi^2\sqrt{2}}\cdot 0.3\approx\pm 0.1\times 10^{-11}. \tag{25}$$

D. First and second generations: logarithmic estimates

In the case of the first generation, i.e., u and d quark loops together with the electron loop, the characteristic hadronic scales are provided by the ρ meson mass, $m_\rho=770$ MeV (for the vector current) and by the a_1 meson mass, $m_{a_1}=1260$ MeV, (for the transversal part of the axial current). Therefore, for Q below m_ρ, only the electron loop contributes to w_T.

On the other hand, the longitudinal part of the axial current is dominated by the π meson whose mass is small. This dominance means that the one-loop expression (18) for $w_L[e,u,d]$ (but not for $w_T[e,u,d]$) works all the way down up to $Q\sim m_\pi$. Thus, the contribution of $w_L[e,u,d]$ in $a_\mu^{\rm EW}$ is strongly suppressed.

Considering $\ln(m_\rho^2/m_\mu^2)$ as a large parameter we see that with logarithmic accuracy the first generation gives for $a_\mu^{\rm EW}$

$$\Delta a_\mu^{\rm EW}[e,u,d]=\frac{\alpha}{\pi}\frac{G_\mu m_\mu^2}{8\pi^2\sqrt{2}}\int_{m_\mu^2}^{m_\rho^2}{\rm d}\,Q^2 w_T^e$$
$$=-\frac{\alpha}{\pi}\frac{G_\mu m_\mu^2}{8\pi^2\sqrt{2}}\ln\frac{m_\rho^2}{m_\mu^2}=-1.08\times 10^{-11}, \tag{26}$$

where we do not differentiate between m_ρ and m_{a_1}.

The case of the second generation, μ,c,s, is more involved. The cancellation of fermion loops takes place at $Q^2>4m_c^2$; so, we take $m_{J/\psi}=3097$ MeV as an upper limit of integration, and $m_\phi=1019$ MeV plays the role of m_ρ for the strange quark. In the interval between m_ϕ and $m_{J/\psi}$ the muon and s quark loops should be included in the integration over Q. In the interval between $m_\eta=547$ MeV and m_ϕ only the muon loop contributes to w_T but we need to account for the pseudo Goldstone nature of the η meson. In contrast to the first generation where the longitudinal part of the axial current had the same quantum numbers as the π meson, we need to reexpress the axial current of the strange quark as a combination of the SU(3) singlet and octet,

$$j_\nu^5[s]=-\bar{s}\gamma_\nu\gamma_5 s=-\frac{1}{3}(\bar{u}\gamma_\nu\gamma_5 u+\bar{d}\gamma_\nu\gamma_5 d+\bar{s}\gamma_\nu\gamma_5 s)$$
$$+\frac{1}{3}(\bar{u}\gamma_\nu\gamma_5 u+\bar{d}\gamma_\nu\gamma_5 d-2\bar{s}\gamma_\nu\gamma_5 s). \tag{27}$$

The singlet part associated with η' does not contribute to w_L below $m_{\eta'}$ (which is of the same order as m_ϕ) but the octet part does, so u, d, and s loops should be taken with octet weights. In the last range, between m_μ and m_η, only the muon loop should be counted. Thus, we arrive at

$$\Delta a_\mu^{\rm EW}[\mu,s,c] = \frac{\alpha}{\pi}\,\frac{G_\mu m_\mu^2}{8\pi^2\sqrt{2}}\Bigg\{\int_{m_\phi^2}^{m_{J/\psi}^2} dQ^2 (w_L[\mu,s] + w_T[\mu,s]) + \int_{m_\eta^2}^{m_\phi^2} dQ^2\left(\frac{2}{3}w_L[s] + \frac{w_L[u]}{3} - \frac{w_L[d]}{3} + w_L[\mu] + w_T[\mu]\right) + \int_{m_\mu^2}^{m_\eta^2} dQ^2 (w_L[\mu] + w_T[\mu])\Bigg\}$$
$$= -\frac{\alpha}{\pi}\,\frac{G_\mu m_\mu^2}{8\pi^2\sqrt{2}} \times\left(4\ln\frac{m_{J/\psi}^2}{m_\phi^2} + \frac{5}{3}\ln\frac{m_\phi^2}{m_\eta^2} + 3\ln\frac{m_\eta^2}{m_\mu^2}\right) = -5.64\times 10^{-11}. \quad (28)$$

To go beyond the logarithmic approximation, we must account for higher powers of $1/Q^2$ for the light quarks. The operator product expansion (OPE), which we next discuss, provides a systematic approach for computing them. It leads to refined estimates of hadronic effects.

E. OPE considerations

At large Euclidean q^2 one can use the OPE for the T-product of electromagnetic and axial currents,

$$\hat{T}_{\mu\nu} = i\int d^4x\, e^{iqx} T\{j_\mu(x) j_\nu^5(0)\} = \sum_i c^i_{\mu\nu\alpha_1\ldots\alpha_i}(q)\mathcal{O}_i^{\alpha_1\ldots\alpha_i}, \quad (29)$$

where the local operators $\mathcal{O}_i^{\alpha_1\ldots\alpha_i}$ are constructed from the light fields. A normalization point μ, which the operators and coefficients implicitly depend on, separates short distances (accounted for in the coefficients c^i) and large distances (in matrix elements of $\mathcal{O}_i$). The field is light if its mass is less than μ. In the problem under consideration this includes the electromagnetic field of the soft photon which can enter local operators in the form of its gauge invariant field strength $F_{\alpha\beta} = \partial_\alpha A_\beta - \partial_\beta A_\alpha$. It also includes gluonic fields as well as lepton and quark fields (with masses less than μ).

The amplitude $T_{\mu\nu}$ is given by the matrix element of $\hat{T}_{\mu\nu}$ between the photon and vacuum states,

$$T_{\mu\nu} = \langle 0|\hat{T}_{\mu\nu}|\gamma(k)\rangle = \sum_i c^i_{\mu\nu\alpha_1\ldots\alpha_i}(q)\langle 0|\mathcal{O}_i^{\alpha_1\ldots\alpha_i}|\gamma(k)\rangle. \quad (30)$$

Since our approximation retains only terms linear in k, the matrix elements are linear in $f_{\mu\nu} = k_\mu e_\nu - k_\nu e_\mu$. This means that only $\mathcal{O}_i$ transforming under Lorentz rotations as (1,0) and (0,1) contribute. In other words, the contributing operators should have a pair of antisymmetric indices, $\mathcal{O}_i^{\alpha\beta} = -\mathcal{O}_i^{\beta\alpha}$. The amplitude $T_{\mu\nu}$ is a pseudotensor so it is convenient to choose $\mathcal{O}_i^{\alpha\beta}$ to be a pseudotensor as well, which is always possible using a convolution with $\epsilon_{\mu\nu\gamma\delta}$. Moreover, the C-parity of $\mathcal{O}^{\alpha\beta}$ should be -1. Retaining only the contributing operators we can write the OPE expansion as

$$\hat{T}_{\mu\nu} = \sum_i \{c_T^i(q^2)(-q^2\mathcal{O}^i_{\mu\nu} + q_\mu q^\sigma \mathcal{O}^i_{\sigma\nu} - q_\nu q^\sigma \mathcal{O}^i_{\sigma\mu}) + c_L^i(q^2) q_\nu q^\sigma \mathcal{O}^i_{\sigma\mu}\}. \quad (31)$$

Parametrizing the matrix elements as

$$\langle 0|\mathcal{O}_i^{\alpha\beta}|\gamma(k)\rangle = -\frac{ie}{4\pi^2}\kappa_i \tilde{f}^{\alpha\beta}, \quad (32)$$

where the constants κ_i depend on the normalization point μ, we get for the invariant functions $w_{T,L}$

$$w_{T,L}(q^2) = \sum c^i_{T,L}(q^2)\kappa_i. \quad (33)$$

1. The leading $d=2$ operator

Operators are ordered by their canonical dimensions d_i which define the inverse power of q in the OPE coefficients. The leading operators have minimal dimensions. In our problem the leading operator dimension is $d=2$,

$$\mathcal{O}_F^{\alpha\beta} = \frac{e}{4\pi^2}\tilde{F}^{\alpha\beta} = \frac{e}{4\pi^2}\epsilon^{\alpha\beta\rho\delta}\partial_\rho A_\delta, \quad (34)$$

where the operator $\tilde{F}^{\alpha\beta}$ is the dual of the electromagnetic field strength, and the numerical factor is chosen in such a way that $\kappa_F = 1$. Its OPE coefficients appear at one loop. Note that this operator corresponds to the unit operator in the product of the three currents in Eq. (14).

In considering the third generation, the normalization point μ can be chosen well below all the masses $m_{\tau,b,t}$, such that the coefficients $c^F_{T,L}$ are given by a one-loop calculation,

$$c^F_{T,L}[\tau,b,t] = w_{T,L}[\tau,b,t], \quad (35)$$

where $w_{L,T}[\tau,b,t]$ are given by Eq. (18) with summation only over $f=\tau,b,t$. Indeed, taking matrix element of $\hat{T}_{\mu\nu}$ we are back to the one-loop expression for the amplitude $T_{\mu\nu}$. Perturbative corrections are governed by $\alpha_s(m_b)$, nonperturbative ones are of order $\sim(\Lambda_{\rm QCD}/m_b)^4$ (due to the operator FGG of dimension 6, see the discussion below).

Such a choice of the normalization point is not possible for the light quarks u,d,s: to apply the perturbative analysis to OPE coefficients we should choose $\mu \gg \Lambda_{\rm QCD}$, i.e., the normalization point μ is certainly much higher than the light quark masses. On the other hand, for $Q \gg \Lambda_{\rm QCD}$ we can choose $\mu \ll Q$. For this range $\Lambda_{\rm QCD} \ll \mu \ll Q$ we can use perturbation theory to calculate the OPE coefficients. In particular, for the leading operator (34) the OPE coefficients $c^F_{T,L}[f]$

in the chiral limit $m_f=0$ are given by the one-loop expressions for $w_{T,L}[m_f=0]$ [see Eq. (20) at $m_f=0$]. An interesting point here refers to dependence on μ for $c^F_{T,L}[m_f=0]$. This dependence is absent not only at the simple level of logarithmic corrections but also at the level of power corrections in μ^2/Q^2.

To demonstrate this let us consider the one-loop calculation of $\hat{T}_{\mu\nu}$ in the background field method. Using the propagator (19) at $m=0$ and doing the spinorial trace we come to the following expression:

$$\int \frac{d^4p}{p^4(p+q)^2}[(p+q)_\mu p^\rho \tilde{F}_{\rho\nu}+(p+q)_\nu p^\rho \tilde{F}_{\rho\mu}], \quad (36)$$

where we have omitted an unimportant overall factor. The integral over Euclidean virtual momentum p is well defined both in infrared and in ultraviolet domains (the logarithmic divergence at large p drops out because of antisymmetry of $F_{\mu\nu}$). It means that the dominant contribution comes from the range of $p\sim q$, since there is no other scale. A simple integration results in

$$\frac{1}{q^2}[q_\mu q^\rho \tilde{F}_{\rho\nu}+q_\nu q^\rho \tilde{F}_{\rho\mu}]. \quad (37)$$

To this one has to add the loop with the massive Pauli-Vilars regulators which is simple to calculate using the propagator (19). This contribution adds a polynomial term $-\tilde{F}_{\mu\nu}$ to the expression (37) that restores the transversality for the electromagnetic current j_μ and leads to the results (20) for $w_{T,L}$ at $m_f=0$.

The calculation above proves that up to power accuracy the OPE coefficients $c^F_{T,L}[m_f=0]=w_{T,L}[m_f=0]$. The portion of the integral (36) which comes from the range $|p|<\mu$ constitutes a correction of order μ^2/Q^2. However, even this correction is absent if the symmetry features of the theory are preserved. Indeed, the polynomial part $-\tilde{F}_{\mu\nu}$ which came from the regulator loop is due to arbitrary short distances so it does not depend on μ at all. The conservation of the electromagnetic current fixes the coefficient between the polynomial regulator part and the dispersive part (37). Separating the part of the integral (36) with $|p|<\mu$ we break the conservation. Moreover, due to chiral symmetry there are no other kinds of corrections, perturbative or nonperturbative, to the one-loop result for the longitudinal coefficient $c^F_L[m_f=0]$. That property is completely valid when we deal with the flavor nonsinglet axial current, like $\bar{u}\gamma_\nu\gamma_5 u-\bar{d}\gamma_\nu\gamma_5 d$ in the first generation, which has no gluonic U(1) anomaly. For the invariant function $w_L[m_f=0]$ that feature follows from the Adler-Bardeen theorem [22] and the 't Hooft matching condition [24]. In terms of the OPE coefficients it translates in the equality of $c^F_L[m_f=0]$ and $w_L[m_f=0]$ because all other OPE coefficients vanish at $m_f=0$ for the longitudinal part.

For the transversal coefficient $c^F_T[m_f=0]$ the situation is more subtle. As shown in [23] the symmetry of the dispersive part (37) under the μ, ν permutation leads to the perturbatively exact relation $2c^F_T[m_f=0]=c^F_L[m_f=0]$. Nonperturbatively this relation is broken at the level of $\Lambda^4_{\rm QCD}/Q^4$ terms as we will see from the OPE analysis.

We can also account for corrections to $c^F_{T,L}$ due to fermion masses which break the chiral symmetry. They can be read off Eq. (20) for $w_{T,L}$. The corrections are of the second order in m_f but logarithmically sensitive to the normalization point μ which replaces m_f under the logarithm in Eq. (20) when we translate to $c^F_{T,L}$,

$$c^F_L[f]=2c^F_T[f]=\frac{4I^3_fN_fQ^2_f}{Q^2}\left[1-\frac{2m^2_f}{Q^2}\ln\frac{Q^2}{\mu^2}+\mathcal{O}\left(\frac{m^4_f}{Q^4}\right)\right]. \quad (38)$$

Summation over f, say for the first generation e,u,d, leads to the lepton-quark cancellation of the leading $1/Q^2$ terms and we must consider operators of higher dimensions.

2. Operators of higher dimension

The next operators, by dimension, are those of $d=3$

$$\mathcal{O}^{\alpha\beta}_f=-i\bar{f}\sigma^{\alpha\beta}\gamma_5 f\equiv\frac{1}{2}\epsilon^{\alpha\beta\gamma\delta}\bar{q}_f\sigma_{\gamma\delta}q^f. \quad (39)$$

Chirality arguments show that their OPE coefficients c^f contain mass m_f as a factor, so by dimension, $c^f\propto m_f/Q^4$. To calculate these coefficients it is sufficient to consider tree diagrams of the Compton scattering type,

$$c^f_L=2c^f_T=\frac{8I^3_fQ_fm_f}{Q^4}. \quad (40)$$

Taking matrix elements between the soft photon and vacuum states we produce the following terms in the invariant functions $w_{T,L}(q^2)$:

$$\Delta^{(d=3)}w_L=2\Delta^{(d=3)}w_T=\frac{8}{Q^4}\sum_f I^3_fQ_fm_f\kappa_f. \quad (41)$$

If we neglect effects of strong interactions, it is simple to calculate κ_f in one loop with logarithmic accuracy using, e.g., the propagator (19) in the external field and the normalization point μ as the UV regulator,

$$\kappa_f=-Q_fN_fm_f\ln\frac{\mu^2}{m^2_f}. \quad (42)$$

Substituting this κ_f in Eq. (41) we observe the full match with the $1/Q^4$ term in Eq. (38), together the $d=2$ and $d=3$ operators reproduce the one-loop $w_{L,T}$ in Eq. (20).

Note that this match is for the terms of second order in mass. In QCD due to spontaneous breaking of chiral symmetry the matrix elements of quark operators (39) are not vanishing at $m_q=0$, instead they are proportional to the quark condensate $\langle\bar{q}q\rangle_0=-(240\ {\rm MeV})^3$. The operators (39) played an important role in the analysis by Ioffe and Smilga

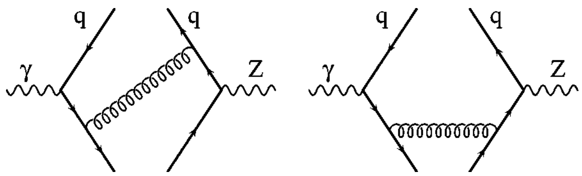

FIG. 4. Diagrams for four-fermion operator $\mathcal{O}_6$.

of nucleon magnetic moments with QCD sum rules [25]. They determined by a sum rule fit the quantity

$$\chi = -\frac{\kappa_q}{4\pi^2 Q_q \langle \bar{q}q\rangle_0} = -\frac{1}{(350\pm 50\ \text{MeV})^2} \tag{43}$$

dubbed as the quark condensate magnetic susceptibility.

Actually, the OPE analysis together with the pion dominance in the longitudinal part leads to a relation for magnetic susceptibility similar to the Gell-Mann–Oakes–Renner (GMOR) relation for the pion mass [26]. This relation derived in Ref. [23] has the form

$$(m_u + m_d)\kappa_q = -m_\pi^2 N_c Q_q . \tag{44}$$

The GMOR relation $F_\pi^2 m_\pi^2 = -(m_u+m_d)\langle \bar{q}q\rangle_0$ allows us to rewrite (44) as

$$\kappa_q = -4\pi^2 Q_q \langle \bar{q}q\rangle_0 \chi, \qquad \chi = -\frac{N_c}{4\pi^2 F_\pi^2} = -\frac{1}{(335\ \ \text{MeV})^2}. \tag{45}$$

Although this value of χ is in a good agreement with the QCD sum rule fit (43) its magnitude is about two times higher than results of other approaches, see [23] for references and discussion.

Let us go further by operator dimensions. Nothing new appears for $d=4$: all operators of dimension 4 are reducible to the $d=3$ operators due to the following relation:

$$\bar{f}(D_\mu \gamma_\nu - D_\nu \gamma_\mu)\gamma_5 f = -m_f \bar{f}\sigma_{\mu\nu}\gamma_5 f. \tag{46}$$

For $d=5$ we have operators $\bar{f}f\tilde{F}^{\alpha\beta}$ and $\bar{f}\gamma_5 f\tilde{F}^{\alpha\beta}$ (with factors m_f again) and at $d=6$ there are many operators of the type $(\bar{f}\sigma^{\alpha\beta}\gamma_5 f)(\bar{f}f)$, $\tilde{F}^{\alpha\beta}\,\mathrm{Tr}\,G_{\mu\nu}G^{\mu\nu}$, and so on. These $d=5,6$ operators produce $1/Q^6$ terms in $T_{\mu\nu}$. A particular example is the following four-fermion operator which appears due to diagrams in Fig. 4:

$$\mathcal{O}_6^{\alpha\beta} = \bar{q}\gamma^\alpha\gamma_5 Q t^a q \bar{q}\gamma^\beta I^3 t^a q - (\alpha\leftrightarrow\beta), \tag{47}$$

where the quark field q has color and flavor indices, the matrices of color generators t^a, $a=1,\ldots,8$ act on color indices, and the weak isospin I^3 and electric charge Q are the diagonal matrices in the flavor space. This operator enters in the OPE (30) with the following coefficients:

$$c_T^6 = -\frac{16\pi\alpha_s(Q)}{Q^6}, \quad c_L^6 = 0. \tag{48}$$

Note that our consideration of four-fermion operators is similar to Ref. [18]. Note also that the operator O_6 contributes only to the transversal function w_T—consistent with the absence of nonperturbative corrections to w_L in the chiral limit. Moreover, in the chiral limit, the $d=6$ operators are next to leading after the leading $d=2$ operator, showing that parametrically the leading nonperturbative corrections are of order $\Lambda_{\mathrm{QCD}}^4/Q^4$.

The matrix element of Eq. (47) between the vacuum and the photon states can be found assuming factorization in terms of the quark condensate $\langle \bar{q}q\rangle_0$ and the magnetic susceptibility κ_q given in Eq. (45). It results in the following piece in w_T for the light quarks in the first (u,d) and second (s) generations,

$$\Delta^{(d=6)} w_T[u,d] = -3\Delta^{(d=6)} w_T[s] = -\frac{32\pi\alpha_s}{9Q^6}\frac{\langle \bar{q}q\rangle_0^2}{F_\pi^2} = -\alpha_s \frac{(0.71\ \ \text{GeV})^4}{Q^6}. \tag{49}$$

We can use this as an estimate for the $1/Q^6$ terms in w_T neglecting the FGG operators which enter with smaller coefficients (they appear in one loop while $\mathcal{O}_6$ is due to tree level diagrams). We also neglect the anomalous dimension of $\mathcal{O}_6$. However, we have in mind that this anomalous dimension is rather large and positive and considerably compensates the running of α_s which therefore can be taken close to 1 for estimates.

Summarizing the consequences of OPE for the u, d, and s quark loops in the chiral limit we get

$$w_L[u,d]_{m_{u,d}=0} = -3w_L[s]_{m_s=0} = \frac{2}{Q^2},$$

$$w_T[u,d]_{m_{u,d}=0} = -3w_T[s]_{m_s=0} = \frac{1}{Q^2} - \frac{(0.71\ \ \text{GeV})^4}{Q^6} + \mathcal{O}\left(\frac{1}{Q^8}\right). \tag{50}$$

The longitudinal part given by the leading $d=2$ operator $\tilde{F}_{\mu\nu}$ has neither perturbative α_s corrections nor nonperturbative ones, and the pole $1/Q^2$ matches the massless pion. So the cancellation of $w_L^{u,d}$ and w_L^e in the first generation is exact in the chiral limit $m_{u,d}=m_e=0$.

As we discussed above the leading operator contribution to the transversal part has no perturbative corrections either [23]; however, nonperturbative corrections are present. Their signal in the chiral limit is very clean: the lowest masses in the vector and axial vector channels are nonvanishing in contrast with the pion in the longitudinal part. In Sec. III F below we present a resonance model for $w_T[u,d]$ consistent with the OPE constraints. Thus, there is no complete cancellation in the sum of $w_T^{u,d}$ and w_T^e although this sum decreases as $1/Q^6$ at large Q.

3. Comparison with the OPE analysis in Ref. [18]

It is convenient at this point to discuss a comparison of our approach with the analysis of the $u,\ d$ quark loops of Ref. [18]. In essence, it is claimed there that the leading large Q behavior of the transversal part $w_T[u,d]$ (and $w_T[s]$ as well) is

$$w_T[u,d]\propto\frac{1}{Q^6}\tag{51}$$

in the chiral limit in contrast with the $1/Q^2$ perturbative behavior. As a result, the $1/Q^2$ part of $w_T[u,d]$ is absent while the $1/Q^2$ part of $w_T[e]$ is present, so the quark-lepton cancellation is destroyed and, consequently, spurious $\log m_Z$ terms appear in $a_\mu^{\rm EW}$.

To pinpoint the origin for such a dramatic difference between our approaches let us notice first that in [18] the authors consider $T_{\mu\gamma\nu}$, the vacuum average of the product of three currents defined in Eq. (14), as a primary object. In this approach they do not have the electromagnetic field entering into local operators and our leading operator $\tilde F_{\alpha\beta}$ does not appear. However, they have to consider the OPE for the product of three currents instead of two. For $T_{\mu\gamma\nu}$ one can derive the following expansion:

$$T_{\mu\gamma\nu}=\langle 0|\sum_i\ c^i_{\mu\gamma\nu\alpha_1\ldots\alpha_i}(q,k)\mathcal{O}_i^{\alpha_1\ldots\alpha_i}(0)$$
$$+i\int d^4y\ \ e^{-iky}T\{\hat T_{\mu\nu}(0)j_\gamma(y)\}|0\rangle.\tag{52}$$

The first part, which contains the local operators, accounts for emission of the soft photon from short distances. The second bilocal part, which contains the operator $\hat T_{\mu\nu}$ defined in Eq. (29) and the soft momentum current j_γ, accounts for the soft photon emission from large distances. Our relation (30) conveniently includes both parts in the local form: the first one is due to operators $\mathcal{O}_i$ containing the electromagnetic field strength $F_{\alpha\beta}$ explicitly and the second is due to the operators without $F_{\alpha\beta}$. Moreover, our leading operator $\tilde F_{\alpha\beta}$ corresponds to the unit operator in the first, local, part on the right-hand side (RHS) of Eq. (52).

Once we have established this correspondence it is simple to see what is missing in the analysis of [18]: they did not account for the local part in Eq. (52). It is the unit operator in this part ($\tilde F_{\alpha\beta}$ in our formalism) which gives the leading $1/Q^2$ contribution and its coefficient follows from the perturbative triangle. This corresponds to soft photon emission from short distances as we discussed above.

Note that the unit operator in the local part of Eq. (52) is leading for both longitudinal and transversal structures in the amplitude $T_{\mu\gamma\nu}$, so its omission should result in an error for the longitudinal contribution as well. This did not happen in [18] because they did not apply the OPE analysis to the longitudinal part of the amplitude, instead fixing it by the anomaly. A comparison with the expansion (52) is particularly simple for the longitudinal part at $m_f=0$: the second bilocal term containing $\hat T_{\mu\nu}$ vanishes and the only surviving operator is the unit operator in the first term.

All the OPE subtleties discussed above should not screen a conceptually very simple situation: the short distance behavior given by free quark loops should not be changed in QCD by large distance effects.

F. First generation

We are now well prepared to calculate the contribution of the first generation to $a_\mu^{\rm EW}$ with an accurate account of hadronic effects. The invariant functions $w_{T,L}$ for the first generation is the sum of $w_{T,L}[e]$, $w_{T,L}[u]$, and $w_{T,L}[d]$. For the electron

$$w_L[e]=2w_T[e]=-\frac{2}{Q^2},\tag{53}$$

where we neglected the electron mass. Expansions at large Q^2 in the chiral limit for $w_{T,L}[u,d]$ are given in Eq. (50). Hadronic effects modify $w_{T,L}[u,d]$. Modifications are minimal for the longitudinal function $w_L[u,d]$: the position of the pole is shifted to m_π^2 due to the explicit breaking of the chiral symmetry by quark masses,[1]

$$w_L[u,d]=\frac{2}{Q^2+m_\pi^2}.\tag{54}$$

To find the contribution of $w_L[u,d]$ to $a_\mu^{\rm EW}$ one needs to use the more accurate Eq. (16), rather than Eq. (17), because the integral is dominated by momenta $Q\sim m_\pi$ comparable with m_μ,

$$\Delta a_\mu^L[e,u,d]=-\frac{\alpha}{\pi}\frac{G_\mu m_\mu^2}{8\pi^2\sqrt2}\left\{2\ln\frac{m_\pi^2}{m_\mu^2}+\frac83+\frac43\int_0^1 d\alpha(1+\alpha)\right.$$
$$\times\ln A+4\frac{m_\pi^2}{m_\mu^2}\left[\int_0^1 d\alpha(1-\alpha)^2\ln A\right.$$
$$\left.\left.-\frac13\ln\frac{m_\pi^2}{m_\mu^2}+\frac29\right]\right\},\tag{55}$$

where $A=\alpha+(1-\alpha)^2(m_\mu^2/m_\pi^2)$. Numerically it gives

$$\Delta a_\mu^L[e,u,d]=-\frac{\alpha}{\pi}\frac{G_\mu m_\mu^2}{8\pi^2\sqrt2}\cdot 2.58=-0.7\times10^{-11}.\tag{56}$$

The transversal function $w_T[u,d]$ can be modeled as a linear combination of two pole terms: one is due to the $\rho(770)$ and $\omega(782)$ vector mesons, another due to the $a_1(1260)$ axial vector meson,

[1]It is just this shift which allows one to derive [23] the expression in Eq. (44) by comparison of the $1/Q^4$ terms with the OPE.

$$w_T[u,d]=\frac{1}{m_{a_1}^2-m_\rho^2}\left[\frac{m_{a_1}^2-m_\pi^2}{Q^2+m_\rho^2}-\frac{m_\rho^2-m_\pi^2}{Q^2+m_{a_1}^2}\right]. \quad (57)$$

The residues in this expression are fixed by two conditions at large Q which follow from the OPE expression (50) plus the $d=3$ terms (41) breaking chiral symmetry. The first condition is on the coefficient of the leading $1/Q^2$ term, the second condition is for the coefficient of $1/Q^4$. The term $1/Q^6$ in Eq. (50) allows for an extra test of the model. The expression (57) gives $-(0.96\ \mathrm{GeV})^4$ to be compared with $-(0.71\ \mathrm{GeV})^4$ in the OPE-based equation (50). Agreement is not extremely good but the right sign and order of magnitude are encouraging. Since the OPE $1/Q^6$ estimate is very approximate, we use Eq. (57) for numerical estimates.

For the integral over Q defining the contribution of $w_T[u,d]$, we can use the simpler expression (17) neglecting m_μ^2/m_ρ^2 corrections,

$$\Delta a_\mu^T[e,u,d]=-\frac{\alpha}{\pi}\frac{G_\mu m_\mu^2}{8\pi^2\sqrt{2}}\times\left\{\ln\frac{m_\rho^2}{m_\mu^2}-\frac{m_\rho^2}{m_{a_1}^2-m_\rho^2}\ln\frac{m_{a_1}^2}{m_\rho^2}+\frac{3}{2}\right\}, \quad (58)$$

which gives numerically

$$\Delta a_\mu^T[e,u,d]=-\frac{\alpha}{\pi}\frac{G_\mu m_\mu^2}{8\pi^2\sqrt{2}}\cdot 4.88=-1.32\times 10^{-11}. \quad (59)$$

Overall, the first generation contributes to a_μ^{EW}

$$\Delta a_\mu^{\mathrm{EW}}[e,u,d]=-\frac{\alpha}{\pi}\frac{G_\mu m_\mu^2}{8\pi^2\sqrt{2}}\cdot 7.46=-2.02\times 10^{-11}, \quad (60)$$

which is to be compared with the constituent quark model result [13],

$$\Delta a_\mu^{\mathrm{EW}}[e,u,d]_{\text{free quarks}}=-\frac{\alpha}{\pi}\frac{G_\mu m_\mu^2}{8\pi^2\sqrt{2}}\left[\ln\frac{m_u^8}{m_\mu^6 m_d^2}+\frac{17}{2}\right]=-4.0\times 10^{-11}. \quad (61)$$

The refined result is about 1/2 of the constituent quark model value. It represents our main phenomenological finding. The primary reason for the shift is a deeper extension into the infrared due to quark-hadron duality for the longitudinal function $w_L[u,d]$. It leads to a stronger quark-lepton cancellation for w_L—the effect noted in Ref. [18].

What is the accuracy of the result (60)? Most of the model dependence is related to the description of the transversal function $w_T[u,d]$. For the longitudinal contribution, the analysis is rather solid. To get an idea of the accuracy, we consider variations when the ρ and a_1 masses are in the intervals 500–1000 MeV and 900–2000 MeV. We found that deviations from the result (60) are within 10%, i.e., of order of $\pm 0.2\times 10^{-11}$. This high level of stability is related to the fact that the main contribution to $\Delta a_\mu^T[e,u,d]$ in Eq. (58) comes from the unambiguous logarithmic term $\ln(m_\rho^2/m_\mu^2)$; it gives -1.08×10^{-11} out of -1.32×10^{-11}.

So, in total, this analysis increases a_μ^{EW} by 2×10^{-11} relative to the free quark calculation and significantly improves its reliability.

G. Second generation

The second generation contains both light s and heavy c quarks which should be treated differently. For the light s quark we use the approach similar to the case of u,d quarks. For the longitudinal function $w_L[s]$, as it was explained above in Sec. III D, one must include both singlet, $\eta'(960)$, and octet, $\eta(550)$, pseudoscalar mesons,

$$w_L[s]=-\frac{2}{3}\left[\frac{2}{Q^2+m_{\eta'}^2}-\frac{1}{Q^2+m_\eta^2}\right]. \quad (62)$$

For the transversal function the model is

$$w_T[s]=-\frac{1}{3}\frac{1}{m_{f_1}^2-m_\phi^2}\left[\frac{m_{f_1}^2-m_\eta^2}{Q^2+m_\phi^2}-\frac{m_\phi^2-m_\eta^2}{Q^2+m_{f_1}^2}\right], \quad (63)$$

where $\phi(1019)$ and $f_1(1426)$ are isoscalar vector and axial vector mesons relevant to the $\bar{s}s$ channel. Integrating $w_{L,T}[s]$ and adding the known expression for the c quark and muon contribution we get for the second generation

$$\Delta a_\mu^{\mathrm{EW}}[\mu,s,c]=-\frac{\alpha}{\pi}\frac{G_\mu m_\mu^2}{8\pi^2\sqrt{2}}\left\{\frac{2}{3}\ln\frac{m_\phi^2}{m_{\eta'}^2}-\frac{2}{3}\ln\frac{m_{\eta'}^2}{m_\eta^2}+\frac{1}{3}\frac{m_\phi^2-m_\eta^2}{m_{f_1}^2-m_\phi^2}\ln\frac{m_{f_1}^2}{m_\phi^2}+4\ln\frac{m_c^2}{m_\phi^2}+3\ln\frac{m_\phi^2}{m_\mu^2}-\frac{8\pi^2}{9}+\frac{56}{9}\right\}. \quad (64)$$

Numerically it constitutes (at $m_c=1.5$ GeV)

$$\Delta a_\mu^{\mathrm{EW}}[\mu,s,c]=-\frac{\alpha}{\pi}\frac{G_\mu m_\mu^2}{8\pi^2\sqrt{2}}\cdot 17.1=-4.63\times 10^{-11}. \quad (65)$$

This numerical value practically coincides with the free quark calculation [13],

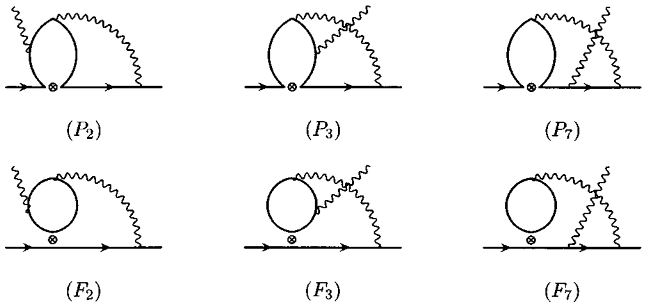

FIG. 5. Mixing of four-fermion operators $V_{\mu f}$, $A_{\mu f}$ with H. The labeling of diagrams follows Ref. [31].

$$\Delta a_\mu^{\rm EW}[\mu,c,s]_{\text{free quarks}} = -\frac{\alpha}{\pi}\frac{G_\mu m_\mu^2}{8\pi^2\sqrt{2}}\left[\ln\frac{m_c^8}{m_\mu^6 m_s^2}+\frac{47}{6}-\frac{8\pi^2}{9}\right] = -4.65\times10^{-11}. \quad (66)$$

Two reasons exist for such a good agreement. First is the smallness of the strange quark contribution—its electric charge is smaller—so, hadronic details are not so important. Second is that the effect of cancellation between leptons and hadrons in the longitudinal invariant function w_L is much less pronounced than in the first generation because of larger masses of η and η'.

The result is more sensitive to the c quark parameters. If we take 1.3 GeV for its mass instead of 1.5 we get $(-4.32)\times10^{-11}$, i.e., a change by 0.3×10^{-11}. Another source of the QCD corrections for the heavy quarks is perturbative gluon exchanges in the quark triangles. This estimation is similar to to one we did in Sec. III C; we substitute $\log m_c$ by $\alpha_s(m_c)/\pi$,

$$\frac{\alpha}{\pi}\frac{G_\mu m_\mu^2}{8\pi^2\sqrt{2}}\cdot 8\frac{\alpha_s(m_c)}{\pi}\approx 0.2\times10^{-11}, \quad (67)$$

where we used $\alpha_s(m_c)\approx0.3$.

We conclude that the uncertainty coming from the second generation is small, about $\pm0.3\times10^{-11}$, and related mainly to charm quark parameters. Overall, the total hadronic loop uncertainties in $a_\mu^{\rm EW}$ are well accounted for by an error of $\pm1\times10^{-11}$.

IV. LEADING LOGARITHMS: RENORMALIZATION GROUP ANALYSIS

It was pointed out in [14] that once the leading logarithm short-distance two-loop corrections to $a_\mu^{\rm EW}$ of order $\ln(m_W/m_\mu)$ are completely known, a renormalization group (RG) analysis can provide all leading logarithm terms of the form $[\alpha\ln(m_W/m_\mu)]^n$, $n=2,3,\ldots$, coming from $n+1$ loop effects. Such an analysis was carried out in Ref. [15] for the leading logarithm three-loop contribution. Since we have now clarified the short-distance two-loop behavior of $a_\mu^{\rm EW}$, it is appropriate for us to revisit the issue of higher orders and refine the previous study.

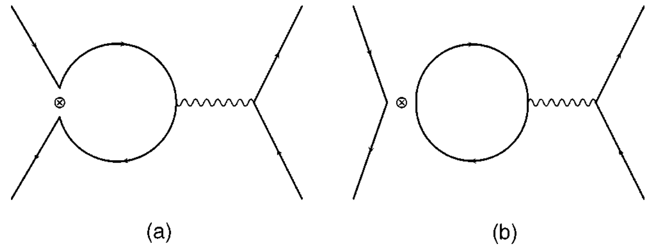

FIG. 6. Renormalization of four-fermion operators: annihilation diagrams.

An interesting subtle feature that enters this RG analysis is the mixing of operators. We are interested in the OPE coefficient of the dimension 5 dipole operator $\bar{\mu}\sigma_{\alpha\beta}\mu F^{\alpha\beta}$. Leading logarithms contribute at the two-loop level due to QED corrections to the dipole operator (its anomalous dimension) as well as from two-loop mixing between the dipole operator and $d=6$, four-fermion operators. A careful treatment of their mixing is important for the RG analysis.

Before addressing the details of $a_\mu^{\rm EW}$, it is useful to recall that a related QCD study was carried out about 25 years ago [27,28] for the case of weak radiative decays which involve flavor-changing gluomagnetic and electromagnetic dipole operators. Indeed, there QCD effects are very large and a RG analysis is essential. Later, because of the phenomenological importance of $b\to s\gamma$, interest in such transition dipole operators increased, generating many studies and some controversies involving subtle issues regarding renormalization scheme dependence, γ_5 definition, operator set completeness, etc. A brief discussion of those issues will provide guidance for our $a_\mu^{\rm EW}$ three-loop analysis.

To discuss the issues that confronted radiative quark decays, we consider the two-loop Feynman diagrams in Fig. 5. These graphs describe mixing of the four-fermion operators, designated by $\otimes$, with the dipole operator. Originally [28] only $P_{2,3}$ and $F_{2,3}$ type diagrams were accounted for. P_7 and F_7 were later calculated in Refs. [29,30] (those authors also accounted for one-loop mixing between gluomagnetic and electromagnetic dipole operators). Numerically, they did not cause much of an effect: about 7% in the mixing coefficients. The smallness of P_7, F_7 is related to the smallness of the internal fermion loop entering as a subgraph, which is basically a part of the photon vacuum polarization operator (it is also nonleading in a $1/N_c$ expansion). The smallness of this fermion loop was used both in [28] and [29,30] to limit the number of four-fermion operators considered to a reduced set. The full set (originally introduced in [28]) contains penguin operators with right-handed fermions that arise from left-handed ones due to the same fermion loop, see Fig. 6. So, their coefficients are also correspondingly small and could be neglected in early studies.

The full operator basis was considered in later publications and we refer to [31] for a discussion of results and references to the literature. There, the renormalization scheme dependence and definition of γ_5 were shown to lead to different four-fermion operators. As explained in [31], to make the definition unambiguous, one has to redefine the four-fermion operators by adding to them dipole operators with appropriate coefficients. Those coefficients are fixed by the requirement that matrix elements of the redefined operators between fermion and fermion plus γ states must vanish. In that way, consistency among different calculational approaches was restored.[2]

Here, we note that the scheme independence can be understood in a simpler way. The basic point is that one-loop subgraphs for the two-loop diagrams in Fig. 5 are finite and unambiguously fixed by the use of gauge Ward identities. A good example is the anomalous fermion triangle involving one axial-vector and two vector vertices where it is well known that the anomaly does not depend on the definition of γ_5. The logarithmic dependence on the normalization point (scale) which comes about due to the second loop integration is then clearly scheme independent. Below, we use this approach, originating from Ref. [28], to calculate all two-loop mixing. The results are consistent with those in Ref. [31] and with the explicit two-loop leading logarithm calculations for a_μ^{EW} given in Sec. II. These consistencies provide a useful check on the analysis.

Our calculation of the two- and three-loop leading logs differ, however, from the results in [15]. The disagreement can be traced to differences in the one- and two-loop anomalous dimension matrix elements. Details are given below.

A. One- and two-loop results

As we discussed in Sec. II the electroweak contribution to the muon magnetic anomaly, $a_\mu = (g_\mu - 2)/2$, can be represented as a sum over W, Z, and Higgs bosons. In the one-loop results the Higgs contribution is negligible and $a_\mu^{\mathrm{EW}}(1\text{-loop})$ given in Eq. (2) is a sum of $a_\mu^{(W)}(1\text{-loop})$ and $a_\mu^{(Z)}(1\text{-loop})$,

$$a_\mu^{(W)}(1\text{-loop}) = \frac{G_\mu m_\mu^2}{8\pi^2\sqrt{2}} \cdot \frac{10}{3},$$
$$a_\mu^{(Z)}(1\text{-loop}) = \frac{G_\mu m_\mu^2}{8\pi^2\sqrt{2}} \cdot \left[-\frac{5}{3}(g_A^\mu)^2 + \frac{1}{3}(g_V^\mu)^2 \right], \tag{68}$$

where we denote the axial-vector and vector couplings of Z to the muon by g_A^μ and g_V^μ. In the standard model,

$$g_A^\mu = 2I_\mu^3 = -1, \quad g_V^\mu = 2I_\mu^3 - 4Q_\mu s_W^2 = 4s_W^2 - 1, \tag{69}$$

and g_V^μ is numerically very small.

At the two-loop level electromagnetic corrections are enhanced by $\log m_Z/m_\mu$. For $a_\mu^{(W)}$, the logarithmic part of the full two-loop result [14] is particularly simple,

$$a_\mu^{(W)}(2\text{-loop})_{LL} = -4\frac{\alpha}{\pi}\ln\frac{m_Z}{m_\mu} a_\mu^{(W)}(1\text{-loop}). \tag{70}$$

[2]We disagree, however, with the statement in [31] about scheme dependence in case of the reduced set of four-fermion operators. In our view it is again related to the definition of four-fermion operators in the full set.

As we discuss below, it just reflects the anomalous dimension of the corresponding dipole operator. In the case of $a_\mu^{(W)}$ it is the only source of the logarithm at two loops.

For $a_\mu^{(Z)}$ the situation is more complicated. In particular, Feynman diagrams without closed fermion loops give [10,14]

$$\begin{aligned} a_\mu^{(Z)}\ (\text{2-loop; no ferm. loops})_{LL} &= \frac{G_\mu m_\mu^2}{8\pi^2\sqrt{2}} \cdot \frac{\alpha}{\pi}\ln\frac{m_Z}{m_\mu}\left[\frac{13}{9}(g_A^\mu)^2 - \frac{23}{9}(g_V^\mu)^2\right] \\ &= -4\frac{\alpha}{\pi}\ln\frac{m_Z}{m_\mu} a_\mu^{(Z)}(1\text{-loop}) + \frac{G_\mu m_\mu^2}{8\pi^2\sqrt{2}} \cdot \frac{\alpha}{\pi}\ln\frac{m_Z}{m_\mu} \\ &\quad \times \left[-\frac{47}{9}(g_A^\mu)^2 - \frac{11}{9}(g_V^\mu)^2 \right]. \end{aligned} \tag{71}$$

In the second line we separated out the piece due to the anomalous dimension.

We also have to add diagrams with closed fermion loops. The diagrams with the muon loops give

$$a_\mu^{(Z)}(\text{2-loop; muon loops})_{LL} = \frac{G_\mu m_\mu^2}{8\pi^2\sqrt{2}} \cdot \frac{\alpha}{\pi}\ln\frac{m_Z}{m_\mu} \cdot \left[-6N_\mu (g_A^\mu)^2 - \frac{4}{9}N_\mu (g_V^\mu)^2 \right], \tag{72}$$

where we introduced the factor N_μ equal to 1 for the muon loop just to distinguish between contributions with and without closed fermion loops. This generalizes calculations in [10,12,13] by including the second term proportional to $(g_V^\mu)^2$ in Eq. (72). This term vanishes at $s_W^2 = 1/4$. In Eq. (72) the first term proportional to $(g_A^\mu)^2$ arises from the induced coupling of a Z with two photons via triangle diagrams, see the diagrams F_2, F_3 in Fig. 5. The second term, from the vector coupling, corresponds to the γ-Z mixing via a muon loop, see the diagram F_7 in Fig. 5.

Fermions other than muons contribute only via closed loops in two-loop order. Including their effect leads to a generalization of Eq. (72) to

$$\begin{aligned} a_\mu^{(Z)}\ (\text{2-loop; ferm. loops})_{LL} &= \frac{G_\mu m_\mu^2}{8\pi^2\sqrt{2}} \cdot \frac{\alpha}{\pi}\sum_f \ln\frac{m_Z}{\{m_f, m_\mu\}} \\ &\quad \times \left[-6 g_A^\mu g_A^f N_f Q_f^2 + \frac{4}{9} g_V^\mu g_V^f N_f Q_f \right], \end{aligned} \tag{73}$$

where we introduced the notation

$$\{m_f, m_\mu\} \equiv \max\{m_f, m_\mu\}. \tag{74}$$

Moreover, Q_f is the electric charge of the fermion, $N_f = 1$ for leptons, and $N_f = N_c = 3$ for quarks, and

$$g_A^f = 2I_f^3, \quad g_V^f = 2I_f^3 - 4s_W^2 Q_f. \tag{75}$$

It is implied that $m_f \ll m_Z$ in Eq. (73); so, it does not include the top quark contribution which is part of the nonlogarithmic, NLL, terms.

The closed loop contribution (73) and the last term in the second line of Eq. (71) are due to the two-loop mixing with four-fermion operators to be discussed below. Overall, the two-loop result for the sum of $a_\mu^{(W)}$ and $a_\mu^{(Z)}$ is [the form is slightly different than Eq. (7) in Sec. II, but equivalent]

$$a_\mu^{(W,Z)}(2\text{-loop})_{LL} = \frac{G_\mu m_\mu^2}{8\pi^2\sqrt{2}} \cdot \frac{\alpha}{\pi}\left\{ -\left[\frac{215}{9} + \frac{31}{9}(g_V^\mu)^2\right]\ln\frac{m_Z}{m_\mu} + \sum_{f=u,d,s,c,\tau,b}\left[6 g_A^f N_f Q_f^2 + \frac{4}{9} g_V^\mu g_V^f N_f Q_f\right]\ln\frac{m_Z}{m_f}\right\}, \tag{76}$$

where we neglected the mass difference between W and Z [the $\ln(m_Z/m_W)$ terms are put into NLL contributions]. The first term in Eq. (76) accounts for diagrams with muons and electrons and in the second term the sum is over all other fermions except the top. The dependence on s_W^2 enters via g_V^μ, g_V^f. Our Eq. (76) differs somewhat from Eq. (25) in [15], as explained at the end of Sec. IV C.

B. Effective Lagrangian

In the effective Lagrangian, represented as a sum over local operators normalized at a point μ, the anomalous magnetic moment of the fermion f is associated with the operator $F_{\alpha\beta}\bar{f}\sigma^{\alpha\beta}f$ of dimension 5. Because of a chirality flip it enters with a coefficient proportional to the fermion mass m_f, and it is convenient to include m_f in the definition of the operator,

$$H(\mu) = -\frac{m_\mu(\mu)}{16\pi^2}[eF_{\alpha\beta}\bar{\mu}\sigma^{\alpha\beta}\mu]_\mu, \tag{77}$$

where the electric charge $e=\sqrt{4\pi\alpha}$ is another factor included in the operator definition. Both the mass m_μ and the electric charge e are μ-dependent quantities in Eq. (77) but the running of the electric charge e is canceled by the wave function renormalization of the electromagnetic strength tensor $F_{\alpha\beta}$. The product $eF_{\alpha\beta}$ is RG invariant.

The effective Lagrangian for flavor and parity preserving transitions can be written as

$$\mathcal{L}_{\text{eff}}(\mu) = -\frac{G_\mu}{2\sqrt{2}}\left\{h(\mu)H(\mu) + \sum_i c^i(\mu)\mathcal{O}_i(\mu)\right\}, \tag{78}$$

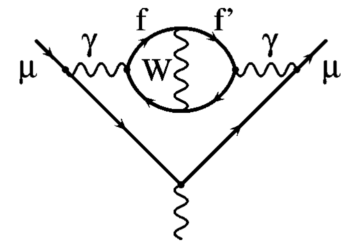

FIG. 7. Contribution to a_μ^{EW} from operators in $\mathcal{L}_W^{d=6}(m_W)$. Both fermions f and f' must be charged so leptons do not contribute.

where the second sum extends over $d=6$ four-fermion operators.[3] The observable value of a_μ^{EW} is related to the coefficient h at the low normalization point $\mu = m_\mu$,

$$a_\mu^{\text{EW}} = \frac{G_\mu m_\mu^2}{8\pi^2\sqrt{2}} h(m_\mu). \tag{79}$$

The relation (79) implies that only the operator H contributes to the matrix elements $\langle\mu|\mathcal{L}_{\text{eff}}(m_\mu)|\mu\gamma\rangle$—a condition that we discussed above.

The one-loop results (68) refer to the range of virtual momenta of order m_W and m_Z, thus fixing the value of h at the high normalization point,

$$h^{(W)}(m_W) = \frac{10}{3}, \quad h^{(Z)}(m_Z) = -\frac{5}{3}(g_A^\mu)^2 + \frac{1}{3}(g_V^\mu)^2. \tag{80}$$

We choose the basis for the four-fermion operators defining them as

$$\mathcal{O}_{V;fg} = \frac{1}{2}\bar{f}\gamma^\nu f \bar{g}\gamma_\nu g, \quad \mathcal{O}_{A;fg} = \frac{1}{2}\bar{f}\gamma^\nu\gamma_5 f\bar{g}\gamma_\nu\gamma_5 g. \tag{81}$$

The $d=6$ part of the effective Lagrangian can be written as

$$\mathcal{L}^{d=6}(\mu) = -\frac{G_\mu}{2\sqrt{2}}\sum_{f,g,\Gamma=V,A} c^{\Gamma;fg}(\mu)\mathcal{O}_{\Gamma;fg}, \quad c^{\Gamma;fg}(\mu) \equiv c_{(Z)}^{\Gamma;fg}(\mu) + c_{(W)}^{\Gamma;fg}(\mu), \tag{82}$$

where $\mathcal{O}_{\Gamma;fg} = \mathcal{O}_{\Gamma;gf}$; so, the OPE coefficients $c^{\Gamma;fg}$ are symmetric under permutation of f and g. The tree-level Z exchange gives the initial data for the OPE coefficients,

$$c_{(Z)}^{\Gamma;fg}(m_Z) = g_\Gamma^f g_\Gamma^g \quad (\Gamma = V,A), \tag{83}$$

where the vector and axial-vector couplings $g_{V,A}^f$ are given in Eq. (75).

In the case of W exchange the tree-level effective Lagrangian is

[3] We omit here the $d=5$ dipole operators for other fermions as well as chromomagnetic dipole operators for quarks, since they do not mix with H.

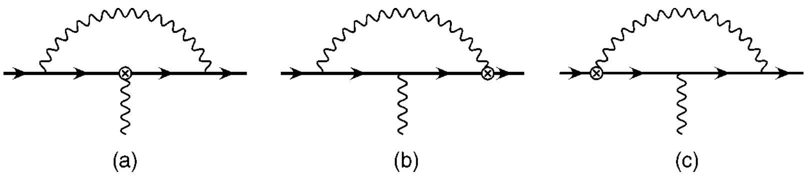

FIG. 8. Anomalous dimension of the dipole operator H.

$$\mathcal{L}_W^{d=6}(m_W)=-\frac{G_\mu}{\sqrt{2}}[\bar{u}\gamma^\nu(1-\gamma_5)d\bar{d}\gamma_\nu(1-\gamma_5)u+(u\to c,d\to s)], \tag{84}$$

where we neglect Cabibbo-Kobayashi-Maskawa (CKM) mixing. Such operators contribute to h only if all fermions are charged, so we can omit the leptonic part (see Fig. 7). One can use the Fierz transformation to put the operator in the following form:

$$\bar{u}\gamma^\nu(1-\gamma_5)d\bar{d}\gamma_\nu(1-\gamma_5)u=\frac{1}{N_c}\bar{u}\gamma^\nu(1-\gamma_5)u\bar{d}\gamma_\nu(1-\gamma_5)d+2\bar{u}t^a\gamma^\nu(1-\gamma_5)u\bar{d}t^a\gamma_\nu(1-\gamma_5)d, \tag{85}$$

where t^a are matrices of the color generators. The part with t^a does not contribute to the magnetic moment (up to gluon corrections which we do not consider here) and neither does the parity breaking part, so $\mathcal{L}_W^{d=6}$ reduces to the form (82) with the initial data

$$c_{(W)}^{\Gamma;ud}(m_W)=c_{(W)}^{\Gamma;du}(m_W)=\frac{1}{N_c}\quad(\Gamma=V,A). \tag{86}$$

There are similar operators and coefficients for u,d substituted by c,s. These are the only operators that contribute to three loop leading logarithm mixing in the W sector.

The renormalization group (RG) equations which allow us to calculate the running of $h(\mu)$ are

$$\mu\frac{\mathrm{d}h(\mu)}{\mathrm{d}\mu}=-\frac{\alpha(\mu)}{2\pi}\times\left[\gamma_H h(\mu)+\sum_{\Gamma,f,g}\beta_{\Gamma;fg}c^{\Gamma;fg}(\mu)\theta(\mu-m_{fg})\right], \tag{87}$$

$$\mu\frac{\mathrm{d}c^{\Gamma;fg}(\mu)}{\mathrm{d}\mu}=-\frac{\alpha(\mu)}{2\pi}\times\sum_{\Gamma',f',g'}\gamma_{\Gamma';f'g'}^{\Gamma;fg}c^{\Gamma';f'g'}(\mu)\theta(\mu-m_{f'g'}), \tag{88}$$

$$\mu\frac{\mathrm{d}\alpha(\mu)}{\mathrm{d}\mu}=-\frac{\alpha^2(\mu)}{2\pi}\sum_f b_f\theta(\mu-m_f),\quad b_f=-\frac{4}{3}N_fQ_f^2. \tag{89}$$

Here γ_H, $\beta_{\Gamma;fg}$, and $\gamma_{\Gamma';f'g'}^{\Gamma;fg}$ form the matrix of anomalous dimensions for operators H and $\mathcal{O}_{\Gamma;fg}$. That matrix is "block triangular": H does not mix with the $d=6$ operators but the operators $\mathcal{O}_{fg}^{\Gamma}$ do mix with H. The $\beta_{\Gamma;fg}$ correspond to these mixings.[4] The θ functions in the RHS count only active fermions at the given μ, with m_{fg} denoting the maximal fermion mass in the operator $\mathcal{O}_{fg}$,

$$m_{fg}=\{m_f,m_g\}\equiv\max\{m_f,m_g\}. \tag{90}$$

Perturbatively $h=h^{(1)}+h^{(2)}+h^{(3)}+\cdots$ where the raised index denotes the number of loops. In one-loop approximation $h^{(1)}(\mu)=h(M)$ where $h(M)$ is given in Eq. (80). In two-loop order one can neglect in the RHS of Eq. (87) the running of α, c_H, and $c^{\Gamma;fg}$, and get

$$h^{(2)}(\mu)=\frac{\alpha(M)}{2\pi}\left[\gamma_H h(M)\ln\frac{M}{\mu}+\sum_{\Gamma,f,g}\beta_{\Gamma;fg}c^{\Gamma;fg}(M)\ln\frac{M}{\{\mu,m_{fg}\}}\right]. \tag{91}$$

Below we will compute γ_H and $\beta_{\Gamma;fg}$ and then verify as a check that Eq. (91) matches the explicit two-loop calculations. We will then use the RG equations (87)–(89) to determine h in three loops.

C. Anomalous dimensions and mixing of effective operators

First, consider the anomalous dimension γ_H of the dipole operator H. It is conveniently computed in the Landau gauge, with a photon propagator $-i(g_{\mu\nu}-k_\mu k_\nu/k^2)/k^2$, since in this gauge there are no logs in Z factors. Thus, γ_H is given by the sum of three diagrams in Fig. 8 minus anomalous dimension $\gamma_m=3$ of the mass $m_\mu(\mu)$ included into the definition (77) of H. The result is

$$\gamma_H=-1-2-2-3=-8, \tag{92}$$

where the numbers correspond to diagrams a, b, c, and $(-\gamma_m)$.

More involved two-loop calculations are needed to determine the mixings $\beta_{\Gamma;fg}$ of the four-operators (81) with H. The relevant diagrams are shown in Fig. 5. It is clear that the operator $O_{\Gamma;fg}$ mixes with H only when at least one of its fermionic indices coincides with the muonic one.

Let us start with operator $\mathcal{O}_{V;\mu f}$ with $f\neq\mu$. It is the diagram F_7 (plus, of course, a similar diagram where the virtual

[4]Note that our definition of anomalous dimensions differs from that in Refs. [31,15] by a factor $(-1/2)$. Also the normalization of four-fermion operators with $f\neq g$ is different.

photon is coupled to the incoming muon leg) which defines $\beta_{V;\mu f}$. The fermion loop in this diagram (which is the same as in the photon polarization operator) produces

$$eN_fQ_f\frac{Q^2}{12\pi^2}\ln\frac{M^2}{Q^2}, \tag{93}$$

where Q is the Euclidean momentum of the virtual photon. The Q^2 factor in Eq. (93) cancels the photon propagator and for the second loop integration we get an expression similar to the one-loop Z boson exchange with the pure vector coupling, $g_V=1$, $g_A=0$, up to the substitution

$$\frac{m_Z^2}{m_Z^2+Q^2}\Rightarrow\frac{e^2N_fQ_f}{24\pi^2}\ln\frac{M^2}{Q^2}. \tag{94}$$

The $\ln(M^2/Q^2)$ can be represented as

$$\ln\frac{M^2}{Q^2}=\int_{\mu^2}^{M^2}\frac{d\tilde{M}^2}{\tilde{M}^2+Q^2} \tag{95}$$

with the range $\mu^2\ll Q^2\ll M^2$. That allows us to get the two-loop result from the one-loop one. From Eq. (80) we see that $h^{(Z)}=1/3$ at $g_V=1$, $g_A=0$. Thus, the diagram F_7 produce

$$\frac{e^2N_fQ_f}{24\pi^2}\cdot\frac{1}{3}\int_{\mu^2}^{M^2}\frac{d\tilde{M}^2}{\tilde{M}^2}=\frac{2}{9}\cdot\frac{e^2N_fQ_f}{16\pi^2}\ln\frac{M^2}{\mu^2} \tag{96}$$

in $h^{(Z)}$. It gives for $\beta_{V;\mu f}$

$$\beta_{V;\mu f}=\frac{4}{9}N_fQ_f,\quad f\neq\mu, \tag{97}$$

where we accounted for another diagram similar to F_7.

For the operator $\mathcal{O}_{A;\mu f}$ with $f\neq\mu$ its mixing with H is given by the diagrams F_2 and F_3. The fermion loop in this case is the anomalous triangle with one axial-vector and two vector vertices. We need its kinematics when the momentum of the external photon tends to zero. The triangle then reduces to [see Eqs. (15) and (20)]

$$\frac{e^2N_fQ_f^2}{2\pi^2}\left[\tilde{F}_{\mu\nu}-\frac{q_\mu q_\sigma}{q^2}\tilde{F}_{\sigma\nu}-\frac{q_\nu q_\sigma}{q^2}\tilde{F}_{\sigma\mu}\right], \tag{98}$$

where q is the momentum of virtual photon and $\tilde{F}_{\mu\nu}=(1/2)\epsilon_{\mu\nu\sigma\delta}F^{\sigma\delta}$ is the dual of the external electromagnetic field $F_{\mu\nu}$. Integration over q in the second loop is logarithmic and produces

$$\beta_{A;\mu f}=-6N_fQ_f^2,\quad f\neq\mu. \tag{99}$$

For the pure muonic operators $\mathcal{O}_{\Gamma;\mu\mu}$ their mixing with H results from diagrams $F_{2,3,7}$ as well as diagrams $P_{2,3,7}$ in Fig. 5. The F diagrams which are due to pairing of fermions from the same current in the four-fermion operators coincide (up to substitutions $N_f\to N_\mu=1$, $Q_f\to Q_\mu=-1$ and the combinatorial factor two due to two ways of pairing) with those of the $\mathcal{O}_{\Gamma;\mu f}$ operators, discussed above.

We can transform the P diagrams, which are due to pairing of fermions from different currents, into F-type diagrams with closed fermionic loops using Fierz transformations,

$$\begin{aligned}\bar{\psi}_1\gamma^\nu\psi_2\bar{\psi}_3\gamma_\nu\psi_4&=\frac{1}{2}\bar{\psi}_1\gamma^\nu\psi_4\bar{\psi}_3\gamma_\nu\psi_2\\&\quad+\frac{1}{2}\bar{\psi}_1\gamma^\nu\gamma_5\psi_4\bar{\psi}_3\gamma_\nu\gamma_5\psi_2\\&\quad-\bar{\psi}_1\psi_4\bar{\psi}_3\psi_2+\bar{\psi}_1\gamma_5\psi_4\bar{\psi}_3\gamma_5\psi_2,\\\bar{\psi}_1\gamma^\nu\gamma_5\psi_2\bar{\psi}_3\gamma_\nu\gamma_5\psi_4&=\frac{1}{2}\bar{\psi}_1\gamma^\nu\psi_4\bar{\psi}_3\gamma_\nu\psi_2\\&\quad+\frac{1}{2}\bar{\psi}_1\gamma^\nu\gamma_5\psi_4\bar{\psi}_3\gamma_\nu\gamma_5\psi_2\\&\quad+\bar{\psi}_1\psi_4\bar{\psi}_3\psi_2-\bar{\psi}_1\gamma_5\psi_4\bar{\psi}_3\gamma_5\psi_2.\end{aligned} \tag{100}$$

We see that the P diagrams can be reduced to already calculated F ones [first two terms in the rhs of Eqs. (100)] and to diagrams of the $F_{2,3}$ type where instead of products of axial-vector currents in the four-fermion operators we have scalar or pseudoscalar ones.

Taken separately, the fermion triangles with the scalar and pseudoscalar vertices contain logarithms and produce double logarithms in the anomalous magnetic moment. But for the difference of scalar and pseudoscalar operators entering Eqs. (100) these double logarithm terms cancel. What remains in this combination can be presented as a piece in the pseudoscalar triangle of the form

$$-\frac{m_\mu}{2\pi^2q^2}q_\sigma\tilde{F}_{\sigma\mu}. \tag{101}$$

The second loop integration is then simple.

Altogether, it results in the following mixings of $\mathcal{O}_{\Gamma;\mu\mu}$ with H

$$\begin{aligned}\beta_{V;\mu\mu}&=-\frac{4}{9}-6+4+2N_\mu\left(-\frac{4}{9}\right)=-\frac{22}{9}-\frac{8}{9}N_\mu,\\\beta_{A;\mu\mu}&=-\frac{4}{9}-6-4+2N_\mu(-6)=-\frac{94}{9}-12N_\mu.\end{aligned} \tag{102}$$

The numbers written after the first equality signs display a decomposition in terms of closed loops: vector, axial-vector and scalar plus pseudoscalar loops. The latter piece has different signs for $\beta_{V;\mu\mu}$ and $\beta_{A;\mu\mu}$. We can unify the expressions (97), (99), and (102) as

$$\begin{aligned}\beta_{V;fg}&=\delta_f^\mu\cdot\frac{4}{9}N_gQ_g+\delta_g^\mu\cdot\frac{4}{9}N_fQ_f+\delta_f^\mu\delta_g^\mu\cdot\left(-\frac{22}{9}\right),\\\beta_{A;fg}&=\delta_f^\mu\cdot(-6N_gQ_g^2)+\delta_g^\mu\cdot(-6N_fQ_f^2)\\&\quad+\delta_f^\mu\delta_g^\mu\cdot\left(-\frac{94}{9}\right).\end{aligned} \tag{103}$$

Now we are well prepared to compare the RG analysis with the explicit calculations of two-loop effects. For the W exchange the two-loop expression (91) reduces to the term with the anomalous dimension $\gamma_H=-8$ which matches the result (70). In the case of $a_\mu^{(Z)}$, inputting in Eq. (91) the initial data (80), (83) and the mixings (103) we observe at $\mu=m_\mu$ full agreement with the sum of Eqs. (71) and (73).

The total two-loop result for $a_\mu^{(W)}+a_\mu^{(Z)}$ given in Eq. (76) differs from that in Ref. [15] in the term $(4/9)g_V^\mu g_V^f N_f Q_f$. In [15] it is multiplied by a factor $(-Q_f)$. This error originated in Eq. (23) of [15] for the two-loop mixing of the operators $V_{\mu f}$ with H. In accordance with the diagram F_7 in Fig. 5, the factor Q_f^2 in that equation should be substituted with $Q_f Q_\mu$.

D. The third loop effect

To determine h at the three-loop level from Eq. (87) we have to account for the running of $\alpha(\mu)$ and $c^{\Gamma;fg}(\mu)$ up to the first loop:

$$\alpha(\mu)=\alpha(M)\left[1+\frac{\alpha(M)}{2\pi}\sum_f b_f\ln\frac{M}{\{\mu,m_f\}}\right], \qquad (104)$$

$$c^{\Gamma;fg}(\mu)=-\frac{\alpha(\mu)}{2\pi}\sum_{\Gamma',f',g'}\gamma^{\Gamma;fg}_{\Gamma';f'g'}c^{\Gamma';f'g'}(M)\times\ln\frac{M}{\{\mu,m_{f'g'}\}}. \qquad (105)$$

Using this expressions as well as the two-loop solution (91) for $h(\mu)$ we find

$$h^{(3)}(m_\mu)=\frac{\alpha^2(M)}{8\pi^2}\Bigg\{\gamma_H h(M)\left[\gamma_H\ln^2\frac{M}{m_\mu}+\sum_f b_f L_f\right] +\sum_{f,g,\Gamma}\beta_{\Gamma;fg}c^{\Gamma;fg}(M)\left[\gamma_H\ln^2\frac{M}{\{m_{fg},m_\mu\}}+\sum_l b_l L_{lfg}\right] +\sum\beta_{\Gamma;fg}\gamma^{\Gamma;fg}_{\Gamma';f'g'}c^{\Gamma';f'g'}(M)L^{fg}_{f'g'}\Bigg\}. \qquad (106)$$

Here

$$L_f=\ln^2\frac{M}{\{m_f,m_\mu\}}+2\theta(m_f-m_\mu)\ln\frac{m_f}{m_\mu}\ln\frac{M}{m_f},$$

$$L_{lfg}=\ln^2\frac{M}{\{m_l,m_{fg},m_\mu\}}+2\theta(m_l-\{m_{fg},m_\mu\})\times\ln\frac{m_l}{\{m_{fg},m_\mu\}}\ln\frac{M}{m_l},$$

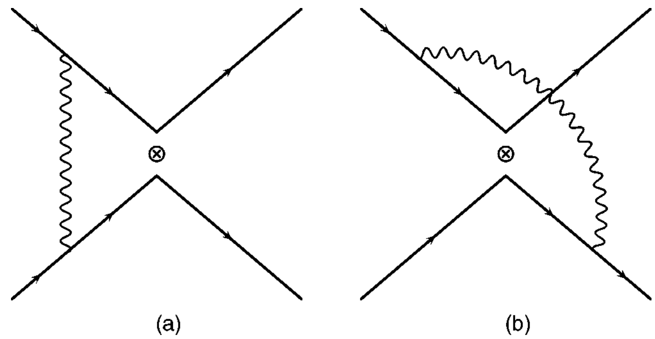

FIG. 9. Renormalization of four-fermion operators: without annihilation.

$$L^{fg}_{f'g'}=\ln^2\frac{M}{\{m_{fg},m_{f'g'},m_\mu\}}+2\theta(m_{f'g'}-\{m_{fg},m_\mu\})\ln\frac{m_{f'g'}}{\{m_{fg},m_\mu\}}\ln\frac{M}{m_{f'g'}}. \qquad (107)$$

Additional input, needed for the calculation of $c_H^{(3)}$, is the anomalous dimension matrix for four-fermion operators. The anomalous dimension matrix $\gamma^{\Gamma';fg}_{\Gamma;f'g'}$ is determined from the one-loop diagrams in Fig. 9 and Fig. 6. The calculations are relatively straightforward: the diagram Fig. 9(b) produces no logarithms in the Landau gauge and can be omitted; the diagram Fig. 6(a) reduces to Fig. 6(b) by means of the Fierz transformations (100). The result for nonvanishing entries in $\gamma^{\Gamma';fg}_{\Gamma;f'g'}$ is

$$\gamma^{V;fg}_{A;f'g'}=-6Q_fQ_g\delta^f_{f'}\delta^g_{g'}-\frac{2}{3}Q_fQ_{g'}\delta^{fg}\delta^f_{f'}-\frac{2}{3}Q_fQ_{f'}\delta^{fg}\delta^f_{g'},$$

$$\gamma^{A;fg}_{V;f'g'}=-6Q_fQ_g\delta^f_{f'}\delta^g_{g'}, \qquad (108)$$

$$\gamma^{V;fg}_{V;f'g'}=-\frac{2}{3}[N_fQ_fQ_{f'}\delta^g_{g'}+N_fQ_fQ_{g'}\delta^g_{f'}+N_gQ_gQ_{g'}\delta^f_{f'}+N_gQ_gQ_{f'}\delta^f_{g'}+Q_fQ_{g'}\delta^{fg}\delta^f_{f'}+Q_fQ_{f'}\delta^{fg}\delta^f_{g'}].$$

Let us now use the expression (106) to calculate the third loop for the W exchange. In this case the effective Lagrangian (84) at $\mu=m_W$ contains only quark operators. They do not mix directly with H so the second term in Eq. (106) does not contribute. In the last term it is the mixing of quark operators with $\mathcal{O}_{V;q\mu}$ which provides a nonvanishing contribution. Another contribution comes from the first term in Eq. (106), associated with the anomalous dimension of H. Using the initial data (86) for $c^{\Gamma;fg}(M)$ after some simple algebra we arrive at

$$h^{(W)}(m_\mu)_{LL}=h^{(1)}_{(W)}+h^{(2)}_{(W)}+h^{(3)}_{(W)}=\frac{10}{3}-\frac{40}{3}\,\frac{\alpha(m_W)}{\pi}\ln\frac{m_W}{m_\mu}+\frac{\alpha^2}{\pi^2}\left\{\frac{10}{3}\left[8\ln^2\frac{m_W}{m_\mu}-\sum_f b_f L_f(M=m_W)\right]-\frac{32}{81}\ln\frac{m_W}{m_Q}\ln\frac{m_W}{m_c}-\frac{32}{81}\ln^2\frac{m_W}{m_Q}\right\}, \tag{109}$$

where we introduced m_Q as an effective IR cutoff for the light quark loops, $q=u,d,s$, implying m_Q is larger then m_μ.[5] We also added the first and second loop to make it easier to follow a numerical comparison. Taking $m_Q=0.3$ GeV, $m_c=1.5$ GeV, $m_b=4.5$ GeV, we get numerically

$$h^{(W)}(m_\mu)_{LL}=h^{(1)}_{(W)}\left[1-26.5\frac{\alpha(m_W)}{\pi}+\frac{\alpha^2}{\pi^2}(352+359-6)\right]=h^{(1)}_{(W)}[1-0.067+0.0038], \tag{110}$$

showing that the third loop effect is quite small. It is dominated by the the anomalous dimension term $\propto\gamma_H^2$ (the first number 352 in α^2 term) and by the cross term $\propto\gamma_H b$ between the anomalous dimension and running of α (the number 359), the four-fermion operators contribute very little, (-6). Moreover, the effect of the third loop becomes even smaller if we use $\alpha(m_\mu)$ instead of $\alpha(m_W)$ in the second loop: this changes the $\gamma_H b$ term in the third loop, $359\to-252$.

Finally, we note that if we shift to the usual fine structure constant, $\alpha=1/137.036$, via the full leading logarithm relation

$$\alpha(m_W)=\alpha+\frac{2\alpha^2}{3\pi}\sum_f N_f Q_f^2\ln\frac{m_W}{m_f}\simeq 1/129, \tag{111}$$

it generates from the $\mathcal{O}(\alpha(m_W))$ terms in Eqs. (109) and (110) additional $\mathcal{O}(\alpha^2)$ contributions that amazingly cancel (numerically) the 0.0038 in Eq. (110). So, in terms of the expansion parameter α, the leading logarithm three-loop corrections are essentially zero. Such a complete cancellation appears to be a numerical coincidence.

The algebra is more tedious in the case of the Z exchange. We set $s_W^2=1/4$ which is a very good approximation numerically. It simplifies the analytic result due to vanishing of the leptonic vector couplings $g_V^{e,\mu,\tau}$ at this value of s_W^2, leaving us with fewer operators. We also combine the W and Z exchanges neglecting the m_W, m_Z mass difference—again quite a good approximation. (The difference will be in the three-loop NLL.)

We present the final result for the three-loop part of $a_\mu^{\rm EW}$ in the form similar to that used in Ref. [15],

$$a_\mu^{W,Z}(3\text{-loop})_{LL}=\frac{G_\mu m_\mu^2}{8\pi^2\sqrt{2}}\cdot\frac{5}{3}\,\frac{\alpha^2}{\pi^2}(A_l+A_q+B_1+B_2), \tag{112}$$

where $A_{l,q}$ come from lepton and quark terms in Eq. (106) containing γ_H^2, $\beta\gamma$

$$A_l=\frac{2789}{90}\ln^2\frac{m_Z}{m_\mu}-\frac{302}{45}\ln^2\frac{m_Z}{m_\tau}+\frac{72}{5}\ln\frac{m_Z}{m_\tau}\ln\frac{m_Z}{m_\mu}, \tag{113}$$

$$A_q=-\frac{2662}{1215}\ln^2\frac{m_Z}{m_b}+\frac{11216}{1215}\ln^2\frac{m_Z}{m_c}+\frac{1964}{405}\ln^2\frac{m_Z}{m_Q}+\frac{24}{5}\ln\frac{m_Z}{m_b}\ln\frac{m_Z}{m_\mu}-\frac{96}{5}\ln\frac{m_Z}{m_c}\ln\frac{m_Z}{m_\mu}-\frac{48}{5}\ln\frac{m_Z}{m_Q}\ln\frac{m_Z}{m_\mu}+\frac{32}{405}\ln\frac{m_Z}{m_b}\ln\frac{m_Z}{m_c}+\frac{32}{135}\ln\frac{m_Z}{m_b}\ln\frac{m_Z}{m_Q},$$

and $B_{1,2}$ are due to the $\gamma_H b$, βb terms involving running of α,

$$B_1=-\frac{179}{45}\left(\frac{1}{3}\ln^2\frac{m_Z}{m_b}+\ln^2\frac{m_Z}{m_\tau}+\frac{4}{3}\ln^2\frac{m_Z}{m_c}+2\ln^2\frac{m_Z}{m_Q}+2\ln^2\frac{m_Z}{m_\mu}\right)+\frac{2}{5}\left(\ln^2\frac{m_b}{m_\tau}+\frac{4}{3}\ln^2\frac{m_b}{m_c}+2\ln^2\frac{m_b}{m_Q}+2\ln^2\frac{m_b}{m_\mu}\right)-\frac{8}{5}\left(2\ln^2\frac{m_c}{m_Q}+2\ln^2\frac{m_c}{m_\mu}\right)+\frac{6}{5}\left(\frac{4}{3}\ln^2\frac{m_\tau}{m_c}+2\ln^2\frac{m_\tau}{m_Q}+2\ln^2\frac{m_\tau}{m_\mu}\right)-\frac{8}{5}\ln^2\frac{m_Q}{m_\mu}, \tag{114}$$

$$B_2=\frac{2}{5}\left[2\ln\frac{m_Z}{m_\mu}+2\ln\frac{m_Z}{m_Q}+\frac{4}{3}\ln\frac{m_Z}{m_c}+\ln\frac{m_Z}{m_\tau}+\frac{1}{3}\ln\frac{m_Z}{m_b}\right]\times\left[\frac{215}{9}\ln\frac{m_Z}{m_\mu}-4\ln\frac{m_Z}{m_Q}-8\ln\frac{m_Z}{m_c}+6\ln\frac{m_Z}{m_\tau}+2\ln\frac{m_Z}{m_b}\right].$$

The B_2 term can be fully absorbed into the two-loop part of $a_\mu^{\rm EW}$ given in Eq. (76) if α there is substituted by $\alpha(m_\mu)$ instead of $\alpha(m_Z)$ which we used in our derivation above.

Comparing with the results in Ref. [15] we see that our B_1 coincides with their B but the sum A_l+A_q is somewhat different from A in [15]. This is due to a few reasons. One was already discussed: in Eq. (23) of [15] for the two-loop mixing of the operators $V_{\mu f}$ with H the factor Q_f^2 should be changed to Q_fQ_μ. In addition, there is a difference in the

[5]Note that in Secs. II and III we used $m_s=0.5$ GeV different from $m_u=m_d=0.3$ GeV but here we make the simplification $m_u=m_d=m_s=m_Q$. That difference has no numerical impact.

one-loop anomalous dimensions of four-fermion operators. In [15] an extra factor 2 is ascribed to the penguin diagrams in Fig. 6. To correct this the factor 1/2 should be introduced in Eqs. (33), (36), (38–41) of [15] and in Eq. (35) the 52/3 should be changed to 44/3.

Numerically,

$$A_l=1696,\quad A_q=-507,\quad B_1=-774,\quad B_2=1916, \tag{115}$$

where we used the same values for the quark masses as above. Altogether, the three-loop correction is

$$a_\mu^{\rm EW}(3\text{-loop})=a_\mu^{\rm EW}(1\text{-loop})\left(\frac{\alpha}{\pi}\right)^2(A_l+A_q+B_1) \simeq 0.4\times10^{-11}, \tag{116}$$

where it is implied that $\alpha(m_\mu)$ is used for the two-loop part. The numerical value is close to that given in [15]. The reason for this final agreement is that the A part of the three-loop result is numerically dominated by γ_H^2 and large mixing of axial operators with the dipole operator, followed by the running of the dipole. These pieces, as well as the B part, are correct in [15]. If $\alpha(m_Z)$ is used in the two-loop part the third loop is somewhat larger, $a_\mu^{\rm EW}(3\text{-loop})\simeq 2.4\times10^{-11}$.

Of course, in both cases one must reevaluate $a_\mu^{\rm EW}$ (2-loop) with the shifted coupling at scale m_μ or m_Z. In that way, scale insensitivity is restored. In addition, because the effective couplings are larger than the usual fine structure constant, α, a transition to this α in the two-loop part of $a_\mu^{\rm EW}$ induces additional negative contributions. Remarkably, those negative contributions cancel with the above explicit three-loop results to about 0.1×10^{-11}. (The cancellation is similar and of course related to the even more complete cancellation pointed out for the W contribution alone.) Hence, to a good approximation, the leading-logarithm higher order contribution is zero or at least negligible.

V. SUMMARY

Having addressed a variety of computational issues including small, previously neglected, two-loop contributions suppressed by factors of $(1-4s_W^2)$ that come from γ-Z mixing and the renormalization of θ_W, strong interaction modifications of quark loop diagrams, and leading logarithm three-loop effects, we are now in a position to update the standard model prediction for $a_\mu^{\rm EW}$ and assess its degree of uncertainty.

Small effects due to γ-Z mixing and our choice of θ_W renormalization have now been included in Eqs. (7) and (8). Because of the $(1-4s_W^2)$ suppression factor, their total impact is rather small, shifting the value of $a_\mu^{\rm EW}$ down by about 0.4×10^{-11}.

More important are strong interaction effects on the quark triangle diagrams in Fig. 3, particularly in the case of light quarks. It was shown that short distance contributions are unmodified (thereby, hopefully, eliminating controversy in the literature). However, QCD can affect their long-distance properties. In the case of the first generation of fermions a detailed operator product expansion analysis and effective field theory calculation led to a shift relative to the free quark calculation (with constituent quark mass) by

$$\Delta a_\mu^{\rm EW}[e,u,d]_{\rm QCD}-\Delta a_\mu^{\rm EW}[e,u,d]_{\text{free quarks}}=+2\times10^{-11}. \tag{117}$$

For the second generation, comparison of the free quark calculation with the more precise evaluation in Eq. (65) shows no significant numerical difference. However, the more refined analysis now indicates very little theoretical uncertainty. So, the total hadronic uncertainties in $a_\mu^{\rm EW}$ would seem to be well covered by an uncertainty of $\pm1\times10^{-11}$ or even less.

Finally, after a detailed renormalization group analysis, the leading logarithm three-loop contributions turned out to be extremely small. In fact, they are consistent with zero, to our level of accuracy $\sim0.1\times10^{-11}$, due to a remarkable cancellation between anomalous dimensions and running coupling effects. Uncalculated three-loop NLL contributions are expected to be of order

$$\frac{G_\mu m_\mu^2}{8\sqrt{2}\pi^2}\left(\frac{\alpha}{\pi}\right)^2\ln\frac{m_Z^2}{m_\mu^2}\simeq 8\times10^{-14}, \tag{118}$$

which is negligible unless enhanced by an enormous factor. Nevertheless, we assign an overall uncertainty of $\pm0.2\times10^{-11}$ to $a_\mu^{\rm EW}$ for uncalculated three-loop NLL contributions.

So, in total we find a small shift in $a_\mu^{\rm EW}$ (for $m_H\simeq150$ GeV) from the previously quoted value of 152(4) $\times10^{-11}$ to a slightly larger (but consistent) value

$$a_\mu^{\rm EW}=154(1)(2)\times10^{-11} \tag{119}$$

where the first error corresponds to hadronic loop uncertainties and the second to an allowed Higgs boson mass range of 114 GeV$\lesssim m_H\lesssim$250 GeV, the current top mass uncertainty, and unknown three-loop effects.

ACKNOWLEDGMENTS

The authors are grateful to S. Adler, S. Eidelman, G. Gabadadze, E. D'Hoker, E. Jankowski, Mingxing Luo, K. Melnikov, M. Shifman, M. Voloshin, and A. Yelkhovsky for helpful discussions. A.V. is thankful for the hospitality to the Aspen Center for Physics where a part of this work was done. We also appreciate communications with G. Degrassi, G. F. Giudice, M. Knecht, S. Peris, M. Perrottet, and E. de Rafael. This research was supported in part by the Natural Sciences and Engineering Research Council of Canada, the DOE grants DE-AC03-76SF00515 and DE-FG02-94ER408, NATO Collaborative Linkage Grant, and the Alexander von Humboldt Foundation.

[1] Muon g-2 Collaboration, G. W. Bennett *et al.*, Phys. Rev. Lett. **89**, 101804 (2002); **89**, 129903(E) (2002).
[2] M. Davier, S. Eidelman, A. Hocker, and Z. Zhang, ''Confronting spectral functions from e^+e^- annihilation and tau decays: Consequences for the muon magnetic moment,'' hep-ph/0208177 v2.
[3] K. Hagiwara, A. D. Martin, D. Nomura, and T. Teubner, Phys. Lett. B **557**, 69 (2003).
[4] K. Fujikawa, B. W. Lee, and A. I. Sanda, Phys. Rev. D **6**, 2923 (1972).
[5] R. Jackiw and S. Weinberg, Phys. Rev. D **5**, 2396 (1972).
[6] G. Altarelli, N. Cabibbo, and L. Maiani, Phys. Lett. **40B**, 415 (1972).
[7] I. Bars and M. Yoshimura, Phys. Rev. D **6**, 374 (1972).
[8] W. A. Bardeen, R. Gastmans, and B. Lautrup, Nucl. Phys. **B46**, 319 (1972).
[9] A. Ferroglia, G. Ossola, M. Passera, and A. Sirlin, Phys. Rev. D **65**, 113002 (2002).
[10] T. V. Kukhto, E. A. Kuraev, A. Schiller, and Z. K. Silagadze, Nucl. Phys. **B371**, 567 (1992).
[11] E. D'Hoker, Phys. Rev. Lett. **69**, 1316 (1992).
[12] S. Peris, M. Perrottet, and E. de Rafael, Phys. Lett. B **355**, 523 (1995).
[13] A. Czarnecki, B. Krause, and W. J. Marciano, Phys. Rev. D **52**, 2619 (1995).
[14] A. Czarnecki, B. Krause, and W. J. Marciano, Phys. Rev. Lett. **76**, 3267 (1996).
[15] G. Degrassi and G. F. Giudice, Phys. Rev. D **58**, 053007 (1998).
[16] A. Czarnecki and W. J. Marciano, Phys. Rev. D **64**, 013014 (2001).
[17] A. Czarnecki and W. J. Marciano, Phys. Rev. D **53**, 1066 (1996).
[18] M. Knecht, S. Peris, M. Perrottet, and E. de Rafael, J. High Energy Phys. **11**, 003 (2002).
[19] S. L. Adler, Phys. Rev. **177**, 2426 (1969).
[20] L. Rosenberg, Phys. Rev. **129**, 2786 (1963).
[21] E. V. Shuryak and A. I. Vainshtein, Nucl. Phys. **B201**, 141 (1982); V. A. Novikov, M. A. Shifman, A. I. Vainshtein, and V. I. Zakharov, Fortschr. Phys. **32**, 585 (1985).
[22] S. L. Adler and W. A. Bardeen, Phys. Rev. **182**, 1517 (1969).
[23] A. Vainshtein, ''Perturbative and nonperturbative renormalization of anomalous quark triangles,'' hep-ph/0212231.
[24] G. 't Hooft, in *Recent Developments In Gauge Theories*, edited by G. 't Hooft *et al*. (Plenum Press, New York, 1980).
[25] B. L. Ioffe and A. V. Smilga, Nucl. Phys. **B232**, 109 (1984).
[26] M. Gell-Mann, R. J. Oakes, and B. Renner, Phys. Rev. **175**, 2195 (1968).
[27] M. A. Shifman, A. I. Vainshtein, and V. I. Zakharov, Zh. Éksp. Teor. Fiz. **72**, 1275 (1977) [Sov. Phys. JETP **45**, 670 (1977)].
[28] M. A. Shifman, A. I. Vainshtein, and V. I. Zakharov, Phys. Rev. D **18**, 2583 (1978); **19**, 2815(E) (1979).
[29] B. Grinstein, R. P. Springer, and M. B. Wise, Phys. Lett. B **202**, 138 (1988).
[30] B. Grinstein, R. P. Springer, and M. B. Wise, Nucl. Phys. **B339**, 269 (1990).
[31] M. Ciuchini, E. Franco, L. Reina, and L. Silvestrini, Nucl. Phys. **B421**, 41 (1994).